M 2014

U.PORTO
FEUP FACULDADE DE ENGENHARIA
UNIVERSIDADE DO PORTO

NANOPARTICLE DRUG DELIVERY SYSTEMS FOR TEMOZOLOMIDE IN THE TREATMENT OF GLIOBLASTOMA

MALINI HONAVAR MELO PIRES

DISSERTAÇÃO DE MESTRADO APRESENTADA
À FACULDADE DE ENGENHARIA DA UNIVERSIDADE DO PORTO EM
ENGENHARIA BIOMÉDICA

FACULDADE DE ENGENHARIA DA UNIVERSIDADE DO PORTO

NANOPARTICLE DRUG DELIVERY SYSTEMS FOR TEMOZOLOMIDE IN THE TREATMENT OF GLIOBLASTOMA

Universidade do Porto

Faculdade de Engenharia

FEUP

Dissertation for Master in Biomedical Engineering

Malini Honavar Melo Pires

Supervisor: Manuel Coelho

Co-Supervisor: Maria do Carmo Pereira

July 2014

“Success is the ability to go from failure to failure without losing your enthusiasm”

— Winston Churchill

ACKNOWLEDGEMENTS

I would mostly like to thank Professor Manuel Coelho for having given me the opportunity to work under his supervision, for his advice, making sure the project was going in a coherent direction, for his kind words and good disposition that was a huge motivation. Professor Maria do Carmo Pereira, my co-supervisor, guided me throughout the year and for that I am immensely appreciative.

There are many people who contributed to the development of my dissertation project. I would like to thank Joana and Barbara for their daily support in the lab, advice and for teaching me the techniques involved for the experiments. I am also grateful to the rest of my colleagues in lab 204A: Maria, Manuela and Silvia for also helping me in the lab.

People in my personal life could not go unmentioned as they have been there for me every day and will surely keep supporting me in my future endeavors. A huge thank you goes to my parents, my grandfather, Rahul and Alberto as well as to all my other friends and family.

The work for this project took place in LEPABE-FEUP and I gratefully acknowledge the funding received by the FCT through the project FCT – PTDC/QUI-BIQ/115449/2009.

ABSTRACT

Temozolomide (TMZ) is an adjuvant chemotherapeutic agent used in the treatment of glioblastoma, in the central nervous system. However, as with all chemotherapeutic drugs, systemic toxicity and side-effects occur. To overcome these limitations and to improve temozolomide efficacy, drug delivery systems were designed based on poly (lactic-co-glycolic acid) (PLGA) nanoparticles and liposomes. The former were produced via the single-emulsion solvent evaporation technique and to produce the latter, the lipid film hydration method was utilized. The nanoparticles were characterized by size through dynamic light scattering and zeta potential (ζ-potential) measurements through laser Doppler velocimetry. The size of PLGA nanoparticles alone was 177 nm, and the ζ-potential was -31 mV; whereas the size of TMZ-loaded PLGA nanoparticles was 176 nm, and the ζ-potential was -2 mV. Liposomes alone showed a size and ζ-potential of 196 nm and -2 mV respectively; whereas TMZ-loaded liposomes showed a size of 195 nm and ζ-potential of -2mV. The stability and the encapsulation efficiency of the systems were evaluated. Although TMZ was found to be adsorbed onto the surface of PLGA nanoparticles instead of being encapsulated within the PLGA nanoparticles, promising results were obtained with liposomes and an encapsulation efficiency of 40-55% was achieved. Liposomes were demonstrated to be a potential nanocarrier for TMZ.

CONTENTS

LIST OF FIGURES

Chapter 2

Chapter 3

Chapter 4

LIST OF TABLES

Chapter 2

Chapter 4

LIST OF ABBREVIATIONS

AIC	5-amino-imidiazole-4-carboxoamide
BBB	Blood-brain barrier
DDS	Drug delivery system
DLS	Dynamic Light Scattering
DNA	Deoxyribonucleic acid
EE%	Encapsulation Efficiency
FR	Folate receptor
GBM	Glioblastoma
MGMT	O^6-methylguanine DNA methyltransferase
MPS	Mononuclear phagocyte system
MTIC	5-(3-methyltriazen-1-yl) imidazole-4-carboxamide
NP	Nanoparticle
PD	Pharmacodynamics
PEG	Poly-ethylene glycol
PGA	Poly (glycolic acid)
PK	Pharmacokinetics
PLA	Poly (lactic acid)
PLGA	Poly (lactic-co-glycolic acid)
PMLA	Poly (β-L- malic acid)
siRNA	Small interfering RNA
Tf	Transferrin
TfR	Transferrin receptor
TMZ	Temozolomide

1. INTRODUCTION

1.1 Motivation

Glioblastoma (GBM) is a highly malignant astrocytoma with an average overall survival rate of 12 months. Current therapy includes radiation and chemotherapy with the adjuvant chemotherapeutic agent temozolomide (TMZ), the latter increasing the overall survival to around 15 months. TMZ as other chemotherapeutic drugs affect both healthy as well as cancerous cells, leading to systemic side-effects and lower bioavailability of the drug in the desired site of action. Lower bioavailability leads to higher doses having to be administered at higher rates, increasing toxicity and often leading to chemotherapy being interrupted. Designing a way to overcome these drawbacks and increase treatment efficacy is therefore of paramount importance. Nanoparticles are being extensively studied as drug delivery systems (DDS) to overcome the limitations of traditional cancer therapies.

Physical or chemical incorporation of the drug into a particulate colloidal system such as liposomes, micro-nanospheres, erythrocytes, polymeric and reverse micelles, are the approaches foreseeable for targeted drug delivery. The design of biocompatible and biodegradable nanocarriers has been developed as an attractive option for DDS. Liposomes and poly(lactic-co-glycolic acid) (PLGA) are both appealing choices for this particular DDS. Liposomes are already available on the market anti-cancer formulations such as liposomal doxorubicin and PLGA is the biodegradable polymer that has been investigated in different formulations. The polymer is approved by the FDA and for several drug delivery systems in humans and is available in different molecular weights and copolymer compositions.

Both Liposomes and PLGA have very different physicochemical, biochemical and mechanical properties each presenting their own advantages where drug delivery is concerned. Functionalization, the addition of ligands specific to the target area increase specificity of the nanoparticle to the affected area. Several molecules selective to brain parenchyma and blood-brain barrier (BBB) have been studied for PLGA and liposomal nanocarriers although no studies have been able to functionalize TMZ-loaded PLGA or liposomes. Therefore, the development of a suitable DDS nanoparticle for TMZ is of high clinical importance.

1.2 Aim

The main objective of this dissertation project was to produce a suitable nanoparticle (NP) drug delivery system (DDS) for temozolomide (TMZ). In order to do this, first, the physicochemical properties of TMZ had to be assessed: stability at different temperatures, pH and behaviour in different solvents. The next step was to produce nanocarriers by using poly (lactic-co-glycolic acid) (PLGA) NPs, and phospholipids (liposomes). After synthesis optimization, TMZ-loaded NPs were produced and characterized by measuring their size, zeta-potential and polydispersity index. The release tests of TMZ from liposomes were performed in PBS for 51 hours.

1.3 Thesis Organization

This thesis is organized into five chapters. Chapter 1 is the Introduction, where a brief explanation of the motivation behind carrying out this particular project, as well as the main objectives for this dissertation are presented. Chapter 2, the State of the art, is a literature review of the following key topics: glioblastoma (GBM); TMZ; PLGA as DDS; liposomes as DDS; NPs already existing for TMZ. In Chapter 3, Material and Methods, the preparation and techniques for characterization of the nanosystems are described. In Chapter 4, Results and Discussion, the main experimental results and achievements are presented and discussed. Finally, in Chapter 5, concluding remarks and future perspectives for the continued research based on this dissertation project are presented.

2. STATE OF THE ART

2.1 Glioblastoma

Glioblastoma (GBM) is a highly malignant tumour of astrocytic lineage in the central nervous system (CNS) and the most common glioma, accounting for 60 to 70% of all the gliomas[2]. Astrocytes, the principal glial cell in the CNS, are responsible for providing structural support, metabolic support to neurons such as supplying nutrients and modulating neurotransmitter function, maintenance and repair of the blood-brain barrier (BBB)[3]. The endothelial cells lining the capillaries in the brain are modified and prevent potentially harmful molecules from entering the brain[4].

Current therapies include surgery and radiotherapy as well as administration of chemotherapeutic drugs including Temozolomide, TMZ. The prognosis of GBM is poor; the median survival is approximately 12 months and less than 3% of patients survive more than 3 years[2,5]. A serious constraint in the treatment of malignant gliomas is the inability to cross the blood brain barrier. However, with improved (targeted) drug efficacy, the overall survival rate may increase and provide the chance for patients to have a better quality of life.

2.2 Temozolomide

Temozolomide (TMZ), a chemotherapeutic agent, has demonstrated activity against glioblastoma and recurrent astrocytomas[5–7]. Adjuvant TMZ chemotherapy with radiation has been shown to significantly improve progression free survival and overall survival in glioblastoma patients, from 12.1 months to 14.6 months. [5] TMZ has the advantage of being able to cross the BBB[8].

Besides being a standard treatment for GBM, TMZ has been used to treat a variety of different neoplasms: advanced malignant neuroendocrine tumours (gastric, thymic, bronchial and pancreatic endocrine); low grade-gliomas; malignant melanoma; aggressive pituitary carcinomas; and recurrent anaplastic oligodendrogliomas [9–12]

2.2.1 Chemical Composition

Temozolomide (TMZ) is also known as Methozolastone, TEMODAR, Temozolamide, as well as 85622-93-1. Its compound ID (CID) is 5394. The molecular formula is $C_6H_6N_6O_2$ with a molecular weight of 194.1 g/mol (structural formula shown in figure 1). The chemical name of temozolomide is 3,4-dihydro-3-methyl-4-oxoimidazo[5,1-d]-*as*-tetrazine-8-carboxamide[13].

Multiple nitrogen atoms in the compound were a key element to design the drug, an imidazotetrazine derivative, in the 1970s. .

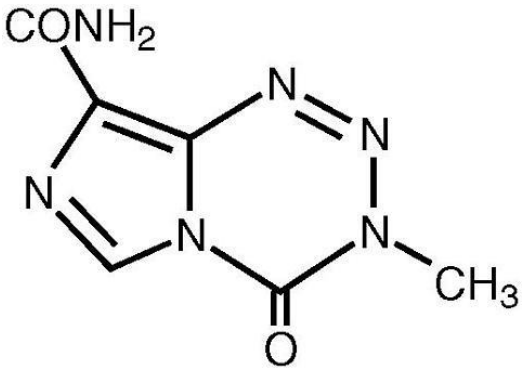

Fig1: Chemical structure of TMZ [Image obtained from [14]]

The compound is a white to light tan/light pink powder, maintaining its stability at acidic pH <5 and labile (readily or continually undergoing chemical, physical, or biological change or breakdown) at pH >7. TMZ is slightly soluble in aqueous solution (2-5mg/ml), acetone, acetonitrile and methanol. It is soluble in dimethyl-sulfoxide (33mg/ml) and very slightly soluble in ethyl acetate and ethanol (0.4-0.6 mg/ml). It has no pKa because it has no functional groups that can be protonated or deprotonated at pH 1-13[15]. Figure 2 presents the Fourier transform infrared spectrum of TMZ. Two strong characteristic bands are observed at 3400 cm^{-1} and 1610 cm^{-1}. The first is due to the N-H stretching mode and the second correspond to the C=C or C=N stretching vibration. TMZ can also be detected through UV-spectroscopy where it has a characteristic peak around 328nm [16,17]. The characteristic UV-Vis spectroscopy peak is shown in Figure 3 below.

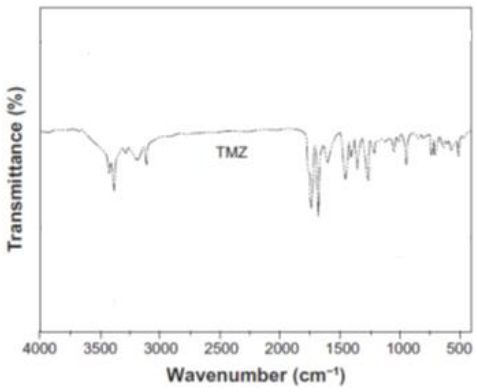

Fig 2 FTIR spectrum of TMZ [18].

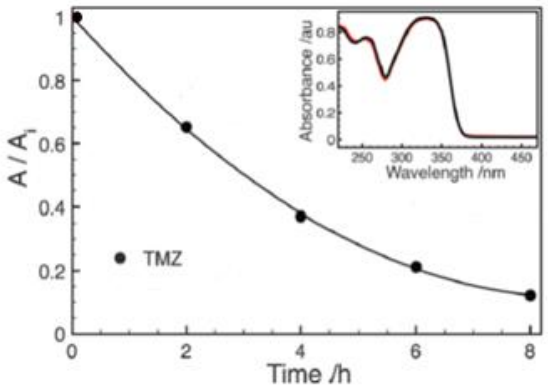

Fig3: UV-vis spectrum of TMZ shows characteristic peak at a wavelength of 328nm. Stability of TMZ in a 10 mM buffer solution at pH 7 showing absorbance of TMZ over time [image adapted from [16]].

2.2.2 Target Site

TMZ can be administered orally and intravenously. It is spontaneously hydrolyzed at physiologic pH to the active component 5-(3-methyltriazen-1-yl) imidazole-4-carboxamide (MTIC). MTIC is then further hydrolyzed to 5-amino-imidiazole-4-carboxoamide (AIC), known to be an intermediate in purine and nucleic acid biosynthesis and into methylhydrazine, the active form responsible for alkylation. Figure 4 shows the chemical structures of TMZ, MTIC and AIC and how the structures are hydrolyzed to produce their respective active components[8].

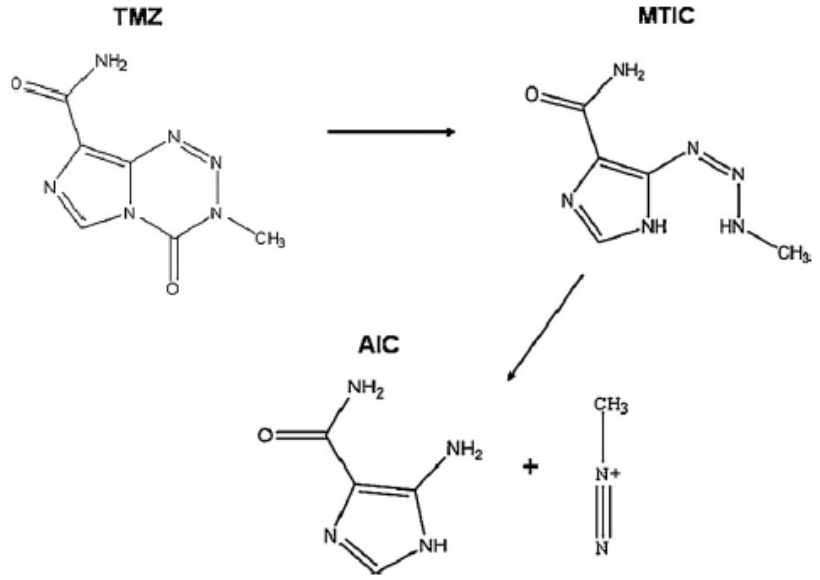

Fig. 4 Chemical Structures of TMZ, MTIC and AIC [8]

2.2.2 Pharmacologic Action

Temozolomide works through the alkylation and crosslinking of DNA. This leads to the eventual degradation of DNA and eventual apoptosis or programmed cell death [19]. TMZ undergoes rapid chemical conversion in the systemic circulation and within cells at physiological pH to the active compound, MTIC. TMZ exhibits schedule-dependent antineoplastic activity by interfering with DNA replication [19] (Figure 5).

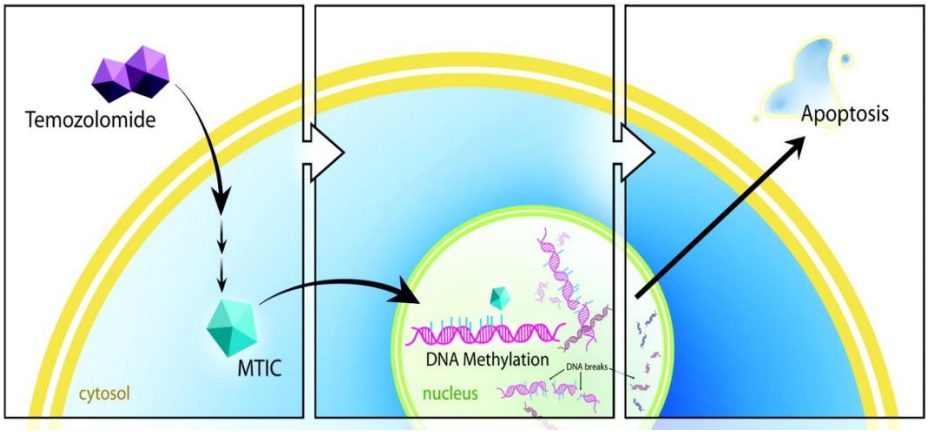

Fig 5.Temozolomide is spontaneously converted to its active form, MTIC. MITC then enters the nucleus passively and alkylates DNA at the O^6 and N^7 positions of guanine. This leads to eventual degradation of DNA and eventual apoptosis of the cell [19].

Absorption, distribution, metabolism and excretion of TMZ throughout the body after administration influence the drug levels and kinetics of drug exposure to the tissues, and this have an impact on the performance and pharmacological activity as a therapeutic agent. In a study, oral TMZ was absorbed rapidly and converted to the active substance, MTIC, and then into AIC. T_{max} values for MTIC were 1.5 to 2 hours after a single dose, and mean T_{max} values for AIC was at 2.5 hours. Peak plasma concentration C_{max} values for MTIC and AIC compared to TMZ were 2.5-4.7% and 13% respectively. The mean area under the plasma drug concentration-time curve (AUC) showed the body exposure to drug after administration of a dose of the drug, varied depending on dose. Mean AUC values ranged from 14.3-15-5 µg.hr/mL for a 100mg/m^2 dose to 176 µg.hr/mL for a 1000 mg/m^2. TMZ shows low protein binding (10% to 20%) and is therefore not likely to interact with high protein bound agents.

Autoradiography data shows a rapid and extensive distribution of ^{14}C-temozolomide to all tissues[20]. The main pathway for excretion was via the kidneys, with only small amounts of radioactivity having been excreted via faeces or via the lungs as CO_2. [20]. After oral administration of ^{14}C labeled TMZ, mean faecal excretion of radioactive C over 7 days was 0.8%. The total recovery of ^{14}C is thought to be low due to the incorporation of AIC into the tissue purine pool. Following oral administration about 5-10% of the dose is recovered unaltered in urine over a period of 24hours, the remainder being excreted as AIC or unidentified polar metabolites [20,21].

2.2.4 Limitations of TMZ in treatment of GBM

GBM is characterized by frequent chemotherapy resistance, in particular to alkylating-based therapies such as TMZ. Resistance to chemotherapy could be either intrinsic (no response to therapy upfront) or acquired (no response following initial response to same therapy). High grade gliomas usually show both intrinsic and acquired resistance, which is most often due to overexpression of the DNA repair enzyme MGMT. The O^6-methylguanine DNA methyltransferase (*MGMT*) gene is encoded on the long arm of chromosome 10, at loci 10q26. O(6)- alkylguanine is the main mutagenic, carcinogenic and cytotoxic lesion in DNA. Tumour expression of the MGMT enzyme is an expression of the methylation status of the promoter region of the *MGMT* gene. Hypomethylated (undermethylated) promoter region of the *MGMT* in tumours, cause an overexpression of the MGMT enzyme and therefore show diminished sensitivity to TMZ. It has been found that approximately 60% of patients with newly diagnosed GBM have a very high MGMT content and thus demonstrate intrinsic resistance to TMZ-based chemotherapy [7]. The treatment of GBM with TMZ is palliative and noncurative; a patient with GBM who receives surgery, radiation therapy and as well as adjuvant chemotherapy regardless of age will have an overall survival of 14.6 months on average[5].

TMZ can induce systemic toxicity including thrombocytopenia, lymphopenia, myelodysplasia. It was reported that 7% of patients who had to discontinue the treatment due to the presentation of these toxic side-effects. This number increased to 14% with patients who were administered TMZ after radiotherapy[5]. When patients present with thrombocytopenia, further chemotherapy cannot be administered safely, requiring frequent transfusions placing patients at risk of long-term bleeding.

TMZ, when compared with other alkylator-based chemotherapies, shows lower toxicity (half to a third as toxic as nitrosoureas), but still has significant toxicity that affects treatment and management of patients with gliomas. Thus, there remains an unmet need for a safe and nontoxic glioma therapy[7].

2.3. Biomaterials already in use for Drug Delivery Systems

The efficacy of conventional chemotherapy is limited due to the difficulty of delivering therapeutic drug concentrations to the target tissue or by their deleterious side-effects on normal tissues and organs. To overcome these restrictions, different approaches have been employed to attempt to use selective delivery to the affected area. The ideal solution would be to target the drug only to the diseased organs, tissues or cells in question.

Colloidal particulates, resulting from physical incorporation of the drug into a particulate colloidal system such as liposomes, micro-nanospheres, erythrocytes and polymeric and reverse micelles, can be suitable for targeted drug delivery. These colloidal particulates are all biocompatible and biodegradable which makes them attractive candidates for drug delivery systems (DDS)[22].

Biodegradable polymers and their respective copolymers are the chosen materials for the manufacturing of a variety of medical and pharmacological devices including DDS for parenteral administration for example. DDS formed on the basis of polymer particles either as nanoparticles (NPs) or as microparticles [23,24]. NPs as DDS have several advantages: particle size and surface can be engineered in order to obtain passive or active drug targeting; drugs can be incorporated without the occurrence of a chemical reaction; drug activity is preserved; different routes of administration can be used to deliver these drugs [23].

Applying DDS in chemotherapy is an attractive option and has been studied for the last few decades in order to increase drug concentration at a specific site and to reduce, often severe, systemic toxicity[23]. This would allow for repeated treatment without concerns about the deposition of the biopolymers or biosynthetic polymers, which could reduce the therapeutic effects.

Structure, properties and applications of nanoparticles are strongly affected by the properties of the polymer used in their formulation. For each application and drug, one must evaluate the properties of the system (drug and particle) and determine the optimal formulation for a given drug delivery application. Polyesters based on polylactide (PLA), polyglycolide (PGA) polycaprolactone (PCL), and their copolymers like poly (lactic-co-glycolic acid) (PLGA), have been widely used as drug delivery systems[24]. Other than use for extended-release pharmaceuticals, PLGA and PLA have also been approved by the FDA for several clinical applications, such as sutures, bone plates and abdominal mesh[24].

2.4 Liposomes as Drug Delivery Systems

2.4.1 What are Liposomes?

Liposomes are vesicles made up of phospholipids. Phospholipids spontaneously form enclosed structures when hydrated in aqueous solutions. These vesicles, made up of one or more phospholipid bilayer membranes, are able to carry drugs of both hydrophilic and hydrophobic nature due to the amphipathic composition of phospholipids. Liposomes possess various properties that make them attractive candidates for DDS. Liposomes, composed of natural phospholipids are biologically inert, are weakly immunogenic and have low intrinsic toxicity. Drugs with different lipophilicities can be encapsulated into liposomes: while strongly lipophilic drugs are entrapped almost completely in the bilayer, strongly hydrophilic drugs are located almost exclusively in the aqueous compartment and drugs with intermediate logP partition easily between lipid and aqueous phases, and can be found in the bilayer as well as in the aqueous core [25,22].

There are several parameters that can be used to classify liposomes: lamellarity (uni-, oligo-, and multi-lamellar vesicles) (figure 6), size (small, intermediate or large) and preparation method. Unilamellar vesicles consist of one lipid bilayer and can have diameters between 50 and 250 nm. They contain a large aqueous core and are used to encapsulate water-soluble drugs. Multilamellar vesicles are composed of an onion-skin-like arrangement made up of many concentric lipid bilayers, having diameters between 1 and 5µm. These multilamellar vesicles, have a high lipid content and can thus passively entrap lipid-soluble drugs[22].

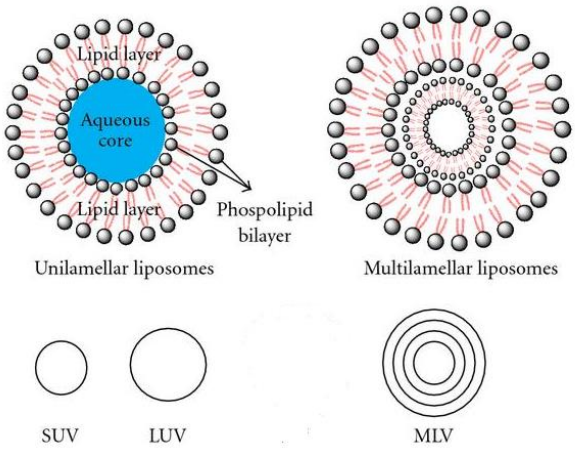

Figure 6: Basic structures of different types of liposomes [22]

Encapsulation of temozolomide in liposomes does not seem to have been done thus far, though studies of liposomal doxorubicin (Calaex) plus temozolomide have been described[27]. However, targeted drug therapy where efficient delivery of liposome-mediated MGMT-siRNA reinforces the cytotoxity of temozolomide in GBM-initiating cells has been described[28]. It has been shown that small-interfering RNA (siRNA)-based downregulation of MGMT could enhance the chemosensitivity of malignant gliomas such as GBM for TMZ. Notably, TMZ-resistant glioma-initiating cells with increased DNA repair and drug efflux capabilities could be efficiently transduced with MGMT-siRNA by using a novel liposome, LipoTrust ™. Thus, these transduced glioma-initiating cells could be sensitized to TMZ in both in vitro and in vivo tumor models[28].

2.4.3 Overcoming Barriers of Conventional Drug Therapy through Liposome DDS

The main problems in drug therapy are biodistribution throughout the body and the targeting of specific receptors. These drawbacks can be overcome by the use of liposomal preparations that protect encapsulated molecules from degradation and that can passively target tissues or organs that have a discontinuous endothelium (e.g the liver, spleen or bone marrow). After intravenous administration, liposomes are quickly captured by the mononuclear phagocyte system (MPS) and removed from the blood circulation [29,30]. This feature has been exploited for therapeutic purposes in order to target diseases like infections located within the MPS, as in the treatment of leishmaniesis with the use of anti-parasitic and antimicrobial drugs[31], and for the encapsulation of immunomodulators in activated macrophages to produce tumoricidal agents in cancer models. When the target site is not the MPS, the uptake of liposomes by macrophages and their consequent removal from circulation is one of the main disadvantages of using of liposomes as a DDS. MPS removes liposomes, by binding to opsonins such as selected serum proteins such as immunoglobbulins, fibronectin beta-2 glycoprotein and C-reactive protein which bind to the surface of liposomes[22].

The complement system, which acts through initiating membrane lysis and enhancing uptake by the MPS cells (monocytes and macrophages) is also able to recognize liposomes. The assembly of C59b-9 complexes (membrane attack complexes, MAC) is able to produce lytic pores which induce the contents of liposomes to be released. On the other hand, serum components that inhibit the phagocytosis of pathogens, dysopsonins, have also been identified. Human serum albumin and IgA possess dysopsonic properties that inhibit

recognition and phagocytosis by the immune system. Regulation of the rate of opsonin clearance has been found to be due to the balance between blood opsonic proteins and suppressive dysopsonic proteins. Another limitation to the stability of liposomes within plasma is the interaction of these with high (HDL) and low density (LDL) lipoproteins. This interaction causes the quick release of the encapsulated drug into the plasma [32,33].

Liposomal physicochemical properties such as net surface charge, hydrophobicity, size, fluidity, and packing of the lipid bilayers all have an impact on the kind of proteins that bind to them and to their overall stability[34,35]. It has been shown that incorporation of cholesterol (CHOL), allows for manipulation of the lipid bilayer through causing the phospholipids to be packed more tightly, which in turn reduces transfer of phospholipids to HDL[36]. Liposomes formed from phosphatidyl choline (PC) that have saturated fatty acyl chains (leading to high liquid crystalline transition temperature) or from sphingomyelin (SM) have been found to be more stable in the blood than liposomes prepared from PC with unsaturated fatty acyl chains[37]. Modulating liposome size and charge is performed in order to reduce uptake by the MPS. The larger the size of the liposome the more rapidly it is cleared from the blood circulation. The half-time of of small unilamellar vesicles (SUVs) is thus longer than that of multilamellar vesicles (MLVs), indicating that phagocytes can distinguish between the sizes of foreign particles. It was therefore deduced that the binding of opsonins to liposomes is dependent on liposome size, and that consequently MPS uptake was also size-dependent [22].

Negatively charged liposomes (with carboxyl groups) prolong half-time of the liposomes in the blood, while positively charged liposomes are toxic and are removed rapidly from circulation [38]. Acidic phospholipids are recognized by scavenger receptors on the surface of macrophages [39]. Surface charge is an important factor in complement system activation by liposomes. In both human and guinea-pig serum, negatively charged liposomes activate the complement system through the classical pathway, while positively charged liposomes activate it via the alternative complement pathway [40].

2.4.3 Functionalization of Liposomes

Overcoming the elimination of liposomes from the blood and capture of the liposomes by cells of the MPS is crucial and several solutions have been developed[22]. The following paragraphs will demonstrate a few of the most common strategies to overcome the barrier of liposome uptake by the MPS.

Immunoliposomes have been developed in order to increase liposomal drug accumulation in the desired tissues and organs. Incorporating surface-attached ligands that are able to recognize and bind to cells of interest has been used to form targeted liposomes. Immunoglobulins (Ig) of the IgG class and their fragments are the most used targeting moieties for liposomes, which can be attached to liposomes without disrupting their integrity or the antibody properties. The IgG is either bonded covalently to the liposome surface or attached through hydrophobic insertion into the liposome membrane after modification with hydrophobic residues [41]. However though there have been significant improvements in targeting efficacy most immunoliposomes accumulate in the liver due to insufficient time for the interaction between the target and targeted liposome to occur. Improved target accumulation can be expected if liposomes can be made to remain in the circulation for a longer period of time [42].

Several techniques have been tested to achieve long circulation of liposomes *in vivo,* through coating the liposomes with inert, biocompatible polymers such as poly-ethylene glycol (PEG). PEG coating forms a protective layer of the liposome surface by slowing down liposome recognition by opsonins and consequent clearance[22]. Such PEGylated liposomes are now being used in clinical practice[22]. These polymers are flexible allowing a small number of such polymer molecules to be grafted onto the liposome surface creating an impermeable layer over the liposome surface. Long-circulating liposomes have been shown to be dose-independent, non-saturable, have log-linear kinetics and an increased bioavailability. Upon PEGylated liposomes accumulating at the target site, through enhanced permeability and retention effect, EPR, where molecules of certain sizes (typically liposomes, nanoparticles, and macromolecular drugs) accumulate in tumor tissue much more (due to higher vasculature and lower lymphatic drainage) than in normal tissues, the PEG is removed due to specific characteristics of the pathological conditions, for example: decreased pH in tumours[22]. Other molecules such as polyvinyl alcohol, poly-N-vinylpyrrolidones and L-amino acid-based biodegradable lipid-conjugates have been found to also provide steric protection of liposomes and thus be used to produce long-circulating

liposomes [43–45]. However, PEGylated liposomes, previously thought to be completely biologically inert were found to activate the compliment system and cause certain side-reactions to take place [46]. Table 1 shows how functionalizing liposomes with specific ligands increases efficacy through targeting specific receptors or properties of the cell.

Table 1: Examples of Ligands that have been bound to liposomes in order to increase specificity of liposomes to target cell

Targetting Moiety	Function	Example	Ref
PEG-Ig or PEG spacer with Ig	Allows for liposomes to be long-circulating increasing bioavailability. Accumulation at target site.	Anti-Her2 liposomes (breast cancer)	22
Folate	Folate receptors (FR) that are over-expressed in tumours. Enter via FR by endocytosis and overcome multidrug resistance; increases cytotixiciy	Folate modified doxorubicin-loaded liposomes (leukaemia; peritoneal tumours)	47 48,49
Transferrin	Targets transferrin-receptor (TfR) on cell receptor- enters cell via receptor-mediated endocytosis. TfR overexpression in cells.	Doxorubicin-loaded liposomes coupled with Tf (glioma cells)	50
Other ligands overexpressed in tumours	Bind to Integrin (Arginylglycylaspartic,RGD); anti-EGFR Ig to bind to bind to overexpressed EGFR in tumour cells; mitomycin C binds to hyaluronan (structural part of extracellular matrix)	Cancer murine models	51,52
pH-sensitive molecules	Liposomes release their contents in response to a decrease in pH inside endosome after endocytosis.	Combination of pH sensitive liposomes with ligand targeting used for both Tf and folate-liposomes.	42

2.4.4 Routes of Administration

There are several routes of administration that are currently being explored for liposomal systems. Administration of liposomes orally requires vesicles to be highly stable, and that the liposomes travel from the gastrointestinal tract to the blood, only beginning release when they are in the blood [53].

Liposomal aerosols were developed after liposome drying methods were established[54]. They were considered an attractive and feasible option for pulmonary drug delivery. Combined aerosol of liposomal paclitaxel and cyclosporin A has shown better outcomes in pulmonary metastases of renal-cell carcinoma in mice than each alone [55]. Delivery of aerosolized liposomes with rifampicin presented better results in the treatment of tuberculosis [56]. Nebulization has been suggested as a delivery mechanism for liposomal aerosols [57,5857,58].

Another route of administration of liposomes is through skin [59]. Different disease models have been explored as targets for topical liposomal drug delivery ranging from skin conditions such as eczema to arthritis and systemic disorders such as diabetes. The efficacy of local anesthetics was enhanced using liposomal delivery. Highly flexible liposomes known as transferosomes, that accompany the trans-epidermal water activity gradient in the skin have been proposed as DDS. Their elasticity permits the vesicles to enter intact skin and to be absorbed into blood circulation[59]. Transferosomes encapsulated with Diclofenac (a non-steroidal anti-inflammatry drug, NSAID), was effective when tested in horses [60]. Liposomes have been used in combination with Iontophoresis (the application of an electric current as a means to enhance the flux of ionic compounds through a membrane such as skin), showing favorable results[61].

Intravenous administration of liposomes, such as doxorubicin-encapsulated liposomes (mentioned earlier) has been combined with radiotherapy for cancer, to enhance therapeutic effect. This combination therapy showed better accumulation of liposomes in the tumour site and increased necrosis of tumour tissue was observed [62].

Liposomes administered subcutaneously have been proposed as a useful tool to target the lymphatic system. The liposomes are carried by lymphatic vessels to the regional lymph nodes where they are taken up by macrophages[63]. Administering biotin and avidin-bound liposomes allows for higher aggregation in macrophages in the lymph node [64].

There is great intra- and interindividual variability in the pharmacokinetics (PK) and pharmacodynamics (PD) of liposomal drugs that complicate their application in clinical practice. Until the drug is released from the liposomal carrier, the PK is only dependent on the liposome. Two groups of factors influence PK/PD, factors associated with the physicochemical properties of liposomes such as size, surface charge and lipid-membrane composition and host factors such as age, gender, body composition and the MPS[65].

2.3.4 New Generation Liposomes

Virosomes are homogeneous spherical unilamellar vesicles, assembled from lipids and purified virus envelope protein[66]. Virosomes were originally developed for intracellular delivery of drugs and DNA, however, subsequently they have been used for the development of new vaccines. Virosomes deliver protein antigens to the immune system, preferentially targeting dendritic cells[66–68]. The only virosome to be clinically tested and commercially available is derived from the influenza virus[66].

Magnetic liposomes, where both drug and a ferromagnetic material are loaded within the nanoparticle, have been developed. When a magnetic field is applied around the target site, the magnetic liposomes accumulate at a higher concentration[69].

Cytoskeleton-specific immunoliposomes have been used in order to target specific tissues. Anti-cardiac myosin monoclonal antibody-bearing liposomes recognize cardiomyocytes with damaged plasma membranes which expose the intracellular myosin. This is used to deliver liposomes to hypoxic cells in myocardial infarcts to assist in repair of the membrane[70].

Liposomes encapsulating human hemoglobin have been developed to enhance oxygen transfer and as a blood substitute[71]. ATP-loaded liposomes have also been developed to protect cells from energy failure or to improve the energy state[72,73]. In photo-dynamic therapy, which is used for tumour ablation, liposomes are used to carry and to enhance photo-sensitizing agents[74].

2.5 PLGA for Drug Delivery Systems

2.5.1 Physico-chemical properties of PLGA

Poly lactic-*co*-glycolic acid (PLGA) is a physically strong, highly biocompatible and biodegradable polymer that has been studied extensively for delivery of drugs (DDS), proteins and other macromolecules [75].

PLGA biodegrades through hydrolysis of its ester linkage. PLGA is considered to be one of the most successfully used biodegradable polymers because its hydrolysis leads to the metabolite monomers, lactic acid, and glycolic acid, which are easily metabolized further by the body via the Krebs cycle [24,76]. Hence, PLGA does not produce systemic toxicity. Figure 7 presents the chemical structure of PLGA. The time needed for the degradation of PLGA is related to the ratio of monomers used in its production. The higher the amount of glycolide

units, the lower the time required for its degradation. However when there is a 50:50 ratio of monomers, degradation occurs at the fastest rate in both in vivo and in-vitro (approximately two months). The degradation rate can then be decreased comparatively when either the lactide or the glycolide units of the copolymer are increased [24].

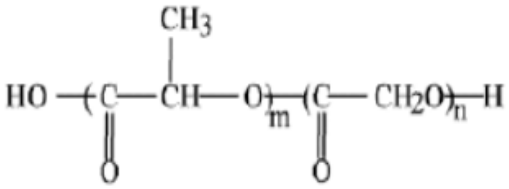

Figure 7: Chemical Structure of PLGA polymer. The "m" component represents lactic acid and "n" component represents glycolic acid [24]

It is known that controlled drug release profiles are provided by changing the PLGA copolymer ratio which affects the crystallinity (low crystallinity and a more amorphous polymer leads to higher degradation rate) of PLGA. If there is a higher ratio of PGA, the crystallinity increases. PLGA of different molecular weights, ranging from 10 kDa to over 100 kDa exist. Molecular weight and copolymer molar ratio influence the degradation process and release profile of the drug entrapped. In general, low molecular weight PLGA have faster degradation rates [24]. Poly (lactic acid) (PLA) contains methyl groups that make it less hydrophilic, absorbing less water and hence copolymers with a high PLA content degrade more slowly than those with a higher Poly (glycolic acid) (PGA) content.

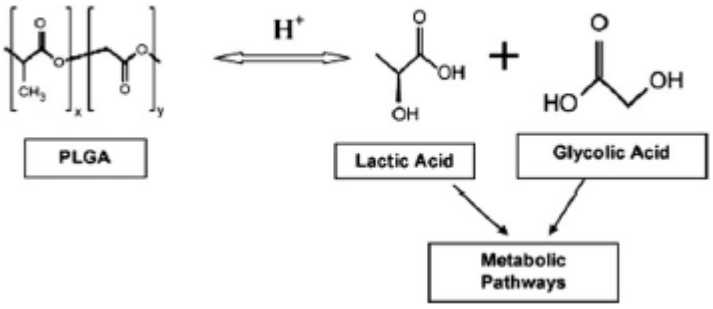

Figure 8: Hydrolysis of PLGA [76]

The drug type can also be a factor that affects the degradation of the polymer. The drug release profile varies considerably depending on the chemical properties of the drug [77]. The amount of drug loaded into the nanoparticle also plays a significant role in the rate of drug releases. A higher drug content, correlates with a larger initial burst release compared to those that have a lower drug content [78]

pH has a strong influence on PLGA hydrolysis, as *in vitro* studies have shown that both alkaline and highly acidic media affect degradation of the polymer. Slightly acidic and neutral media however, do not show such effects[79].

It has been hypothesized that although PLGA degrades primarily via hydrolytic degradation, enzymatic degradation of PLGA may also occur. However this has not yet been confirmed *in-vivo* [80,81].

PLGA is the biodegradable polymer that has been investigated the most [82]. The polymer is approved by the FDA and European Medicine Agency (EMA) for several drug delivery systems in humans and is available in different molecular weights and copolymer compositions[1]. Depending on all the factors mentioned above, the degradation time can vary from several months to several years [83], one of its most favorable characteristics. It is this has a slow rate of degradation, which governs the rate at which the loaded drug is released. For example, FDA approved drug formulations such as that for recombinant growth hormone, used in the treatment of paediatric growth hormone deficiency (GHD), developed in 1999, requires only one or two doses a month compared to conventional therapy which required multiple doses per week [82].

2.5.2 Internalization of PLGA NPs

PLGA NPs are internalized through fluid phase pinocytosis and also through clathrin-mediated endocytosis. After cellular internalization (via endocytosis) the PLGA NPs undergo a surface charge reversal (anionic to cationic) due to the acidic pH of endo-lysosomes destabilization of late-endossomal membrane allowing efflux of NP and drug release[84] as shown in figure 9.

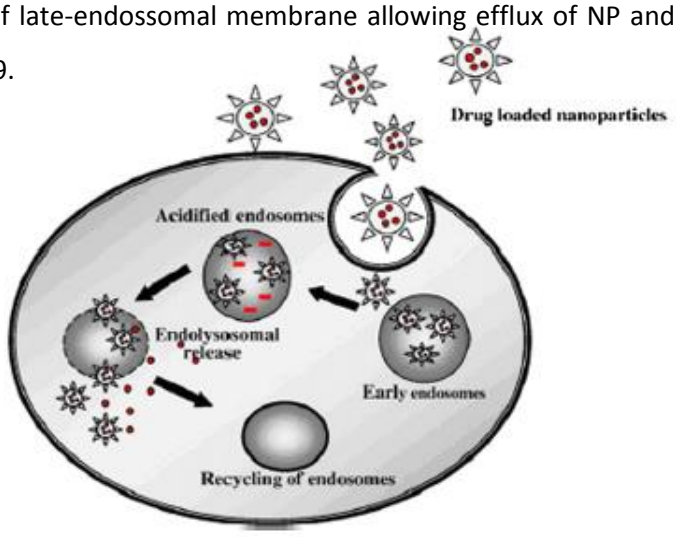

Figure 9: Schematic representation of NP internalization in cells and rapid release of drug from endosomes[85].

2.5.3 Synthesis of PLGA Nanoparticles

Several methods have been devised to syntheise PLGA nanoparticles depending on the physico-chemical characteristics of the drug to be encapsulated. The most common is the emulsification- solvent evaporation technique.

Single emulsion solvent evaporation process

This technique is used for the encapsulation of hydrophobic drugs. It consist in dissolving PLGA and the drug in an organic solvent such as dichloromethane (DCM), ethyl acetate (EÄ) to form a single phase solution. This organic solution is then emulsified by using water containing a surfactant (Polysorbate 80, Polaxamer 180, Pluronic F127 *etc*.) to form an oil-in-water (O/W) emulsion. The nanosized droplets are formed by sonication. The organic solvent is then evaporated and the nanoparticles collected upon centrifugation [86–88].

Double emulsion solvent evaporation process

This technique is used to encapsulate hydrophilic drugs. First, the drug is dissolved in an aqueous phase and then added to the organic phase containing PLGA and stirred vigorously to produce the water-oil (W/O) emulsion. This emulsion is added to an aqueous solution containing a surfactant and further emulsified to form the water-oil-water (W/O/W) emulsion followed by sonication of the emulsion. The organic solvent is then evaporated and the nanoparticles collected upon centrifugation [86–88].

In emulsion solvent evaporation techniques choice of solvent and stirring rate are crucial to the encapsulation efficiency and final particle size [1]. Also, different sources use different emulsifying agents. Polyvinyl alcohol (PVA) has been said to be used frequently to form more uniform NPs that are smaller in size and are easy to redisperse in aqueous medium at the end of the procedure [89].

Nanoprecipitation

Another technique nanoprecipitation or interfacial deposition method, where polymer and drug are dissolved in an organic solvent such as acetone and added dropwise into water or allowed to dialize out into the aqueous phase the organic solvent is evaporated and the nanoparticles collected after centrifugation. The advantages of this technique is that it allows for both hydrophilic and hydrophobic molecules to be encapsulated and is a relatively simple technique[90].

2.5.4 Application of PLGA as DDS: What is already available?

PLGA NPs hold huge potential in applications combining targeting, imaging, diagnostics and therapy [91]. Conjugation, where drug remains adsorbed to surface, as well as encapsulation of drugs in PLGA systems decreases the limitations of the drugs such as short circulation half-life and non-site specific targeting. The latter leads to undesirable systemic side effects, particularly those of the highly toxic compounds used for the treatment of malignant disease. PLGA DDS increase the *in-vivo* circulation time substantially and also reduce endocytic cellular uptake [92].

Table 2: Summary of Examples of DDS PLGA systems developed mostly in the areas of cancer and brain disease.

	DDS (kind of NP)	Functionalization	Application	Studies
CANCER	PLGA- (Doxorubicin)	cLABL	A549 lung epithelial cells (cancer) *In-vitro*	[93]
	PLGA- (Paclitaxel)	None but coated Cremophor EL Stabilizer	Wide range of cancers (brest, lung, Ovary and leukaemia) clinical use	[94]
	PLGA- (Paclitaxel)	AS1411 DNA aptamer which binds to nucleolin in plasma membrane	Anti-glioma drug delivery *In-vivo*	[95]
	PLGA- (Paclitaxel)	RGD-PEG	Targets $\alpha_v\beta_3$	[96]
	PLGA- (Doxorubicin)	PEG	Anti-tumoural; *In-vitro*	[97,98]
	PLGA-(Doxorubicin)- Au	Au	As the PLGA NPs biodegraded, DOX was released, and heat was locally generated upon near-infrared (NIR) irradiation due to NIR resonance of DOX-loaded-Au NPs.	[99]
	PLGA- (Paclitaxel)	Folate	Targets folate receptors in cancer Cells; *in-vivo, in-vitro*	[100]
	PLGA- (Doxorubicin)	Folate- Vitamin E	Targets folate receptors and improves drug permeability across cell membranes *In-vivo, in-vitro*	[101]
INFLAMMATION	PLGA-(Dexamethasone)	-	Occular delivery for uveitis and other eye infections. *in-vitro*	[102]
CEREBRAL DISEASES	PLGA-(superoxide dismutase)	-	Increases BBB permeability, more efficient against oxidative stress in cerebral ischemia, restoration of neurological functions after stroke. Preclinical (mice)	[103]
	PLGA (urocortin)	Lactoferrin	Binds to lf receptors in the BBB facilitating its passage through it. Used for Parkinson disease; Preclinical	[104]
	PLGA-(loperamide)	Simil-opioid peptide, sialic acid	Allows anti-nociceptive drug to cross BBB. Remains in brain parenchyma. Preclinical	[104–107]

2.5.5 PLGA DDS developed for TMZ

TMZ is the drug of choice used in the treatment of GBM. Due to its very short half-life of 1.8hrs and adherence of proteins to its surface, repeated administration of the drug is required. Systemic side-effects as well as lack of site-specificity, meaning that the amount of drug reaching the tumour site is limited, are further drawbacks.

Recently, a variety of approaches have been tested and applied in order to enhance the loading of TMZ into materials such as PLGA. PLGA has been used as a microparticle for coating TMZ [108,109]. Zhang et al 2012 encapsulated TMZ with hydroxyapatite nanocrystals (nHA) under different morphological conditions, rod-shaped and spherical, to test differences in loading capacities and the efficacy of drug release. The in-vitro drug release assay showed that TMZ/PLGA/nHA microspheres have a much slower burst release rate of TMZ compared to TMZ/PLGA due to the nHA, which plays an important role in the process of TMZ controlled release [108]. Moreover, their study also showed that the use of nHA as an additive helped both in the release of TMZ from microspheres to occur, and in inhibiting glioma growth and invasion when tested *in vitro* with the U87 glioma cell line. Ultimately, the TMZ/PLGA/nHA microspheres have shown the best performance in TMZ controlled release as well as in inhibition of cell viability. Therefore TMZ/PLGA/nHA microspheres show potential as drug delivery carriers for glioma therapy [108]. However, there is an important limitation of this DDS, as the microspheres are approximately 60µm in diameter, an extremely large size for crossing the BBB. It is known that particles capable of crossing the BBB and thus entering the brain must be smaller than 200nm [110]. The study also shows high encapsulation efficiencies, defined as the percentage of the actual mass of drug encapsulated in the polymeric carrier in relation to the initial amount of drug loaded, (EE% >80%) with a very high initial burst rate even though the nHA decreased it significantly. One may assume that a lot of the TMZ was adsorbed on the surface of the microsphere.

Zhang & Gao studied TMZ-loaded PLGA microparticles and their antitumour effects against Glioma C6 cancer cells[109]. The single emulsion solvent evaporation technique was used, using dichloromethane as the organic phase and PVA as the emulsifying agent (saturated with TMZ beforehand in addition to adding TMZ to the organic phase). Parameters investigated included different polymer/solvent ratios (W/V%) ranging from 5 to 13.33 as well as different stirring rates of the emulsion (400, 600 and 800 rpm), and different TMZ:PLGA mass ratio (5%-40%). EE% was shown to be higher using lower TMZ: PLGA ratios and microparticle size was approximately 60µm in all experiments. Higher stirring rate correlated with smaller particle size. Though there was a high initial burst of

TMZ in the first day, results showed sustained release over 35 days. Cytotoxicity results showed that TMZ-loaded PLGA decreases cell viability percentage significantly in comparison to PLGA alone, but results for cytotoxicity studies with TMZ alone are not presented, which is crucial for assessing the efficacy of the system.

Jain et al. studied the cytotoxicity of temozolomide loaded into PLGA nanoparticles[111]. In contrast to the two studies mentioned above the NPs of 150-160nm were developed using the solvent diffusion method (a modification of the solvent-emulsion evaporation method [111]) using acetonitrile, a partially miscible organic solvent and a TMZ:PLGA mass ratio of 60% and zeta potential of the NPs was around -20mV. 30% of the loaded TMZ was released within the first 2hours but there was sustained release of the drug over the following 120 hours. The IC50 for the pure drug was only concentration dependent (at 72 h and 96 h IC50 was 150µg/mL) whereas for the encapsulated drug NP the IC50 was both concentration and time dependent due to variations in release rates of the drug at different time-points (at 72 h and 96 h IC50 was 200µg/mL and 150µg/mL). Other tests: cell motility, clonogenic potential, observation of changes in cellular morphology upon TMZ and PLGA NP treatment, flow cytometry and immunofluorescence to visualize internalization were performed to further prove the efficacy of the system. The latter two experiments, showed higher uptake of TMZ/PLGA NPs into the cells in comparison to FITC a hydrophilic molecule, concluding that the uptake of a hydrophilic or amphipathic molecule (TMZ) would be enhanced by the use of PLGA [110].

Although the study by Jain et al. shows promising results, it would however be interesting to know how the IC50 varied at a wider range of time-points. Also, they only test their DDS on one glioma cell line. Testing this formulation on both cancer cells and normal astrocytic cells because since these particles are not targeted, may show very different results in non-neoplastic astrocytic cell lines (due to differences in morphology and epigenetic profile), and therefore testing cytotoxicity in these cells is crucial before proceeding to *in-vivo* models. Also, because Jain et al, use a relatively high TMZ:PLGA mass ratio, it would be of interest to test a range of these to see which is more effective in terms of EE% and differences in size of particle as well as zeta potential and polydispersity. Another aspect which could be explored is the stability of the NPs over time as the zeta potential of approximately -20 mV and flocculation of the molecules could occur over time if the NPs are stored for a longer period of time (more than 5 days). Hence further studies to develop TMZ loaded PLGA nanoparticles should be undertaken to both corroborate with the few available studies and to try to improve the efficacy of the system.

3. MATERIALS AND METHODS

3.1 TMZ Stability Tests

TMZ, Selleckchem (Munich, Germany), dissolved in PBS (solubility 0.33 mg/mL) at 10 µg/mL and UV-spectrum measured at hourly intervals over 36 hours at 22 °C and 37 °C and at pH 7 through spectrophotometry. After acidifying a 10 µg/mL to a pH of 5.6 with 0.02 M HCl solution, and its stability measured over 36 hours again. pH was measured with an H1 110 series pH meter (Hanna® Instruments, USA) and UV-vis spectrum was measured with BioTek® Synergy 2 high-performance multi-mode plate reader.

A TMZ solution at 10 µg/mL at pH 7.24 was used and increased pH was achieved by the addition of 0.02M NaOH solution. Solutions at pH 11.2, pH 11.9 and pH 12.3 were measured.

Measurements were taken at room temperature using spectrophotometry with the BioTek® Synergy 2 high-performance multi-mode plate reader at 22 °C in triplicate.

The stability test was also conducted with the same materials but at differing temperatures: 22 °C (room temperature) and 37 °C (physiological body temperature).

3.2 TMZ Solubility in Different Solvents

TMZ is an amphiphilic molecule according to the literature[15,18]. To study the solubility, TMZ was dissolved in an array of different polar and organic solvents: water, acetone, chloroform, ethyl acetate, dichloromethane and dimethyl sulfoxide: all at 10 µg/mL, concentrations much below their saturation concentration. Each solution was measured in triplicate using the UV-1700 PharmaSpec UV-Vis spectrophotometer from Shimadzu (Japan).

3.3 TMZ Calibration Curve

To produce a linear calibration curve of TMZ dissolved in PBS, solutions were prepared at 0, 2, 5, 10 and 20 µg/mL (equivalent to 0, 10.3, 25.8, 51.5, 103 µM). UV-spectrum absorbance at wavelengths 255 nm-266 nm (MTIC/AIC) and 328 nm (TMZ) was measured and recorded in triplicate and two calibration lines were set for each respective wavelength. Since spectrophotometry was used with both BioTek® Synergy 2 high-performance multi-mode plate reader and UV-1700 PharmaSpec UV-Vis spectrophotometer from Shimadzu (Japan), two separate calibration curves were obtained to take into consideration differences in sensitivity of the devices (Appendix A1 and A2).

To produce liposomes, TMZ dissolved in PBS was left overnight to transform completely into its degradation products that have only one peak at the 255-266 nm region when measured by spectrophotometry. It was decided that this would simplify quantification of the drug for more prolonged experiments involving nanoparticles such as the release experiments (used for TMZ-loaded liposomes). Therefore all experiments for liposomes were used with the degradation products of TMZ, and quantified with a calibration curve produced with a range of concentrations from 0, 5, 10, 15, 20, 30, 40, 50 µM, latter is quantity of drug required to be encapsulated in liposomes, (equivalent to 0, 0.97, 1.94, 2.91, 3.88, 5.82, 7.77 and 9.71 µg/mL). UV-1700 PharmaSpec UV-Vis spectrophotometer was used to obtain these measurements (Appendix A3).

3.4 Nanoparticle Production

3.4.1 Materials for Nanoparticle Preparation

For PLGA nanoparticle preparation, a solution of 1%(w/v) Pluronic F127 was prepared using Pluronic® F127 purchased from Sigma–Aldrich (St. Louis, Mo., U.S.A). PLGA Resomer® RG503H (50:50; MW = 24.000 – 38.000) and ethyl acetate were also obtained from Sigma–Aldrich (St. Louis, Mo., U.S.A). TMZ from Selleckchem (Munich, Germany). Dimethylsulfoxide (DMSO) was purchased from Sigma-Aldrich (Germany). Deionized ultrapure water was used to prepare Pluronic F127 solutions.

For liposome production, lipids were purchased from Avanti Polar Lipids: DSPC (1,2-distearoyl-*sn*-glycero-3-phosphocholine, MW 790.145), Chol (cholesterol ovine wool, MW 386.65), DSPE-PEG2000 (1,2-distearoyl-*sn*-glycero-3-phosphoethanolamine-N-[amino(polyethylene glycol)-2000] ammonium salt), MW 2790.49). Each of these reagents were dissolved in chloroform. TMZ solution was prepared in Phosphate buffered saline (PBS) at different concentrations. PBS solution was prepared in deionized ultrapure water (Milli-Q Academic, Millipore, France).

3.4.2 PLGA NPs: Method of Preparation

To synthesize PLGA NPs, the single-emulsion solvent evaporation technique was used[80-88]. A 70 µL solution of 142.86mg/mL Resomer® RG503H of PLGA in ethyl acetate (10 mg), was prepared, and for encapsulation purpose a 30 µL solution of 16.67 mg/mL and 33.33 mg/mL (0.5 mg and 1 mg respectively) of TMZ was added to DMSO. The suitable masses of TMZ, PLGA polymer and pluronic F127 were weighed in a NewClassic MS Analytical Balance from Mettler Toledo (Switzerland).

200 µL of an aqueous solution of 1% (w/v) pluronic F127 was added dropwise to the organic phase (PLGA and TMZ dissolved in ethyl acetate). The mixture was then vortexed (Genius 3, ika®vortex, Germany) for 30 seconds and emulsified by sonication in a beaker with ice using Ultrasonic cleaner (VWR™, Malaysia) for 5 minutes at 45 kHz.

After emulsification, the mixture was poured rapidly into 2.5 mL of 0.1% (w/v) pluronic F127 and stirred (800 rpm) at room temperature for 3 hours, to completely evaporate the organic solvents (DMSO and ethyl acetate), using a magnetic stirrer. It is of utmost importance that this step is completed very quickly in order to avoid PLGA NP aggregation before being stabilized by the surfactant. Evaporation took place in a flow chamber Captair®bio from Erlab (Barcelona, Spain).

The suspension was then filtered with Millex-GP Filter Units (0.2 µm, polyethersulfone) (Millipore Express, Ireland) and incubated overnight at 4°C to prevent NPs from aggregating and

to increase their stability. The NPs were collected by centrifugation (14500 rpm, 30 min) with MiniSpin®plus Eppendorf, Germany). The resulting pellet of NPs was re-suspended in 1 mL of ultrapure water and stored for analysis. The supernatant was also saved for quantification purposes (i.e- encapsulation efficiency). The method is seen in figure 10.

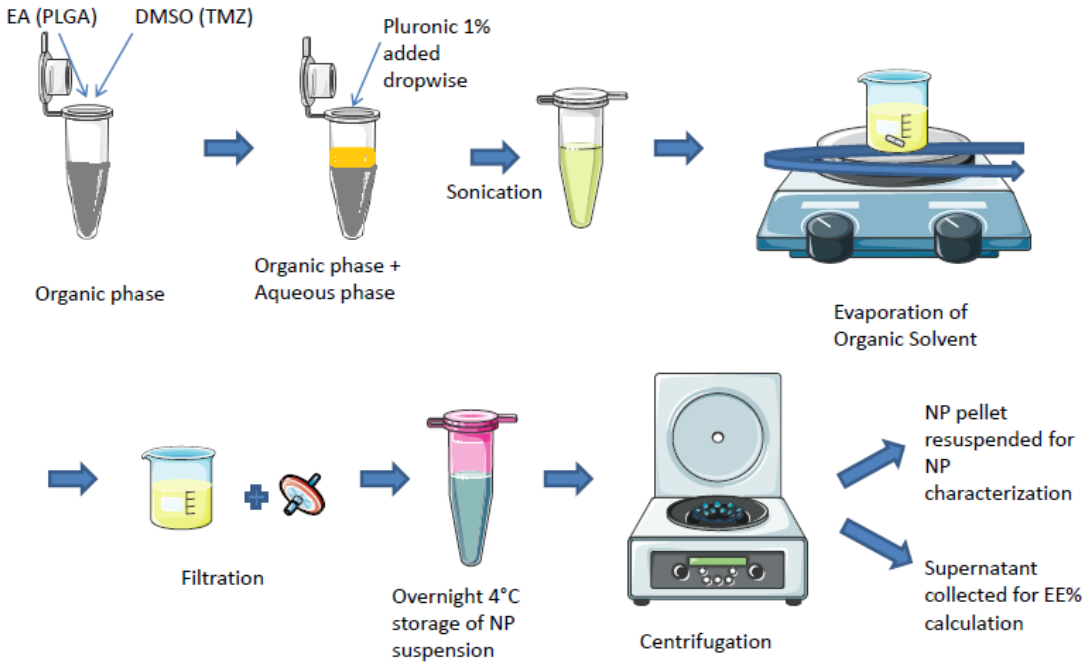

Fig 10: PLGA NP production method.

Modifications to the Method

The method was carried out as above but substituting the surfactant pluronic F127 with polysorbate 80 obtained from Sigma-Aldrich (St. Louis, Mo., U.S.A) in the same (w/v) percentages as described above for pluornic F127.

The method was also carried out as above but was produced with 0.5 mg of TMZ instead of 1 mg (produced at half PLGA/TMZ loading percentage).

3.4.3 Liposomes: Method of Preparation

To prepare the liposomes, the lipid film hydration method was used. DSPC, Chol and DSPE-PEG2000 were mixed in a molar ratio of 52:45:3 into a glass flask. The chloroform solvent was evaporated by drying with a stream of nitrogen gas while rotating the flask so as to form a lipid film. The flask was left in vacuum overnight to ensure that all the chloroform evaporated. The lipid film was hydrated by adding PBS or PBS/TMZ (for liposomes alone or liposomes with TMZ respectively) to obtain a final lipid concentration of 0.8 mM. Ratio of TMZ to lipids was 1:16. The mixture was then vortexed for 15 min to obtain MLVs. To form LUVs, the suspension was then treated to 10 cycles of freezing and thawing followed by extrusion 11 times through a polycarbonate filter of 200 nm. In order to measure the efficiency of encapsulation, a PD-Midi Trap G25 (GE Healthcare) column was used to separate the encapsulated TMZ from free TMZ molecules, eluting only the liposomes. To quantify the amount of TMZ inside the liposomes, the nanoparticles were burst with both ethanol and sodium dodecyl sulphate (SDS) purchased from Sigma-Aldrich (Germany), in a 25:75 (v/v) proportion. Figure 11 shows the method step-by-step.

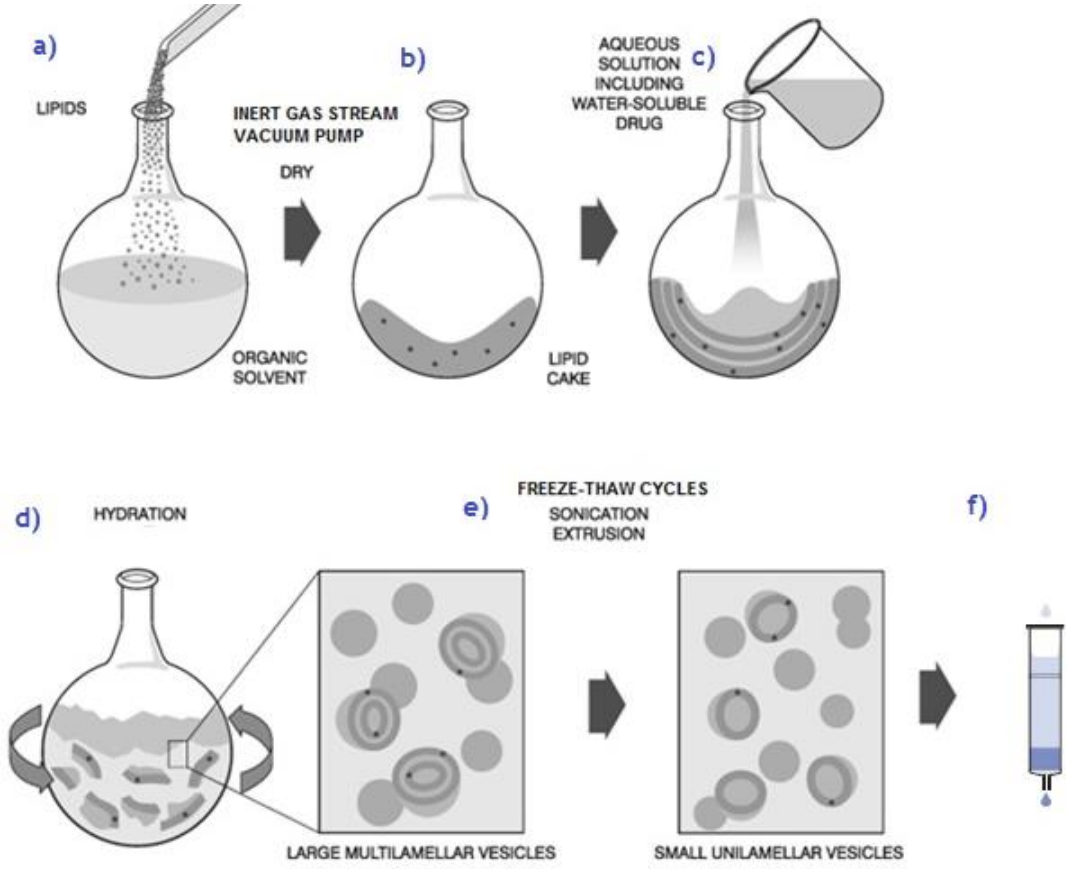

Fig 11: Liposome production steps: a) Lipid mixture in organic chloroform (DSPC, cholesterol, PEG); b)drying with stream of nitrogen gas; c)hydration with PBS or TMZ/PBS solution and d) vortexing; d) freeze-thaw cycles and extrusion; and e) separation of non-encapsulated TMZ from encapsulated TMZ NPs through desalting column [image adapted from [112]].

3.5 Nanoparticle Characterization

For both PLGA NPs and liposome NPs, the size, polydisperisty index and zeta potential were measured using the ZetaSizer NanoZS, Malvern Instruments (Worcestershire, UK).

3.5.1 Dynamic light scattering technique: size and polydispersity

DLS is a technique used to characterize particles, emulsions or molecules which are either dispersed or dissolved in a liquid. The Brownian motion of particles or molecules in suspension causes scattering of laser light at different strengths. By analyzing these changes in intensity, the velocity of the Brownian motion and hence particle size can be determined through the Stokes-Einstein relationship[113]. Particle size is given in terms of hydrodynamic

radius. The (*d(H)*) is the diameter of a sphere that has the same translational diffusion coefficient as the particle. It is a hypothetical sphere that moves identically as the particle that is being measured.

$$d(H) = \frac{kT}{3\pi\eta D} \quad \textbf{[1]}$$

Where: *D* is the diffusion coefficient; *η* is viscosity in the medium; *k* is the Boltzmann's constant; and *T* is the absolute temperature. Brownian diffusion depends on the following parameters: temperature, viscosity and size of the NP. The higher the temperature, the faster the movement; the higher the viscosity, the slower the movement and if nanoparticles increase in size movement is slower[114,115].

To measure NP average size (in both liposomes and PLGA NPs) the measurements were performed using disposable cuvettes obtained from Sarstedt (Germany) and using PBS and water as the dispersant medium. Triplicate measurements were made and for each measurement, 12 runs were performed at 25°C.

The Polydispersity Index (PdI) is a measure of the width of the particle size distribution. The formula for Polydispersity is $PdI = (\sigma / d)^2$, where the polydispersity (PdI) = the square of the standard deviation (σ) / mean diameter (d) [116]. Polydispersity indices lower than 0.1 are typically referred to as "monodisperse". DLS also measured PdI when measurements for NP average size were made. DLS was measured on the day of NP production as well as over time to look out for changes in size and polydisperisty.

3.5.2 Zeta Potential through Laser Doppler Velocimetry

Laser Doppler Velocimetry (LDV) also called Laser Doppler Electrophoresis (LDE) allows the zeta potential to be determined through obtaining the value for electrophoretic mobility and then applying a mathematical model[117].

Ions in proximity to the surface of the particle will be strongly bound while ions that are further away will be lightly bound forming what is called a diffuse layer. Within the diffuse layer there is a boundary and any ions inside this boundary will move with the particle when it moves in the liquid; but any ions outside the boundary will stay where they are – this boundary is called the Slipping plane. A potential exists between the particle surface and the dispersing liquid which varies according to the distance from the particle surface – this potential at the slipping plane is called the zeta potential (ζ-potential or ZP). LDV measures the velocity of a particle in a

liquid when an electrical field is applied. The applied electric field causes the particle to move in relation to a stationary liquid at a constant velocity. The ratio of the velocity to the electric field, *E,* is the electrophoretic mobility, μ. The mobility is converted into zeta potential, ζ, using the Smoluchowski equation:

$$\xi = 4\pi \frac{\eta \mu}{D} \quad \textbf{[2]}$$

where η is the viscosity of the suspension, D is the dielectric constant of the solution and μ is the electrophoretic mobility of particles (micrometer/s per volt/cm)[118].

The value of the zeta potential gives an indication of the stability of the colloidal system. If all the particles in suspension have a large negative or positive zeta potential then they will tend to repel each other and there is no tendency to flocculate. On the other hand, if the particles have low zeta potential values then there is no force to prevent the particles coming together and flocculating[117].

ZetaSizer used to measure the zeta potential of the NPs in suspension. Capillary cells from Malvern (Wostershire, UK) were used and the dispersant was both water and PBS. Each NP suspension was measured in triplicate, each measurement having had 12 runs. Zeta potential was measured on the day of NP production and then later measured over time to see if any changes in ZP value were observed.

3.5.3 Encapsulation Efficiency (EE%) of PLGA NPs

To quantify the amount of TMZ encapsulated in the NPs, the supernatant collected after the centrifugation was diluted 10x and UV-Vis spectrum of the sample was measured, and concentration of unloaded TMZ was calculated according to the calibration curve. The EE% was calculated through the following formula:

$$\boldsymbol{EE\%} = \frac{\boldsymbol{Total\ amount\ of\ TMZ - Unloaded\ amount\ of\ TMZ}}{\boldsymbol{Total\ amount\ of\ TMZ}} X\ 100$$

[3]

3.5.4 Encapsulation Efficiency (EE%) of Liposomes

The drug quantified upon bursting with sodium dodecyl sulfate (SDS), showed a peak in the characteristic UV-Vis region, indicative of drug entrapment. To obtain an approximate concentration of how much drug was present upon bursting of the liposome, another calibration curve was made for the degradation products alone.

The following formula was used to calculate the encapsulation efficiency:

$$EE\% = \frac{Amount\ of\ drug\ inside\ nanoparticle}{Total\ amount\ of\ drug}\ X\ 100$$

[4]

3.6 Release Study of TMZ-loaded Liposomes

TMZ-loaded liposomes were used for drug release experiment by using a dialysis membrane (Float-A-Lyzer G2, CE, 100 KDa, SpectrumLabs). The drug alone was used as a control in one membrane and the drug encapsulated in the liposomes was used in another membrane. The membranes were washed in ultrapure water for 12 hours before being used and equilibrated with buffer 1 hour before the dialysis with PBS buffer as the receiving phase. A volume of 2.5 mL from the liposomes and TMZ suspensions was added to their respective membrane and the outside space was filled with 2.5 mL of buffer. The dialysis membrane was kept in continuous stirring at 200 rpm at 37 °C to simulate physiological conditions. Samples were collected from the outside medium over and the quantity of released TMZ was determined by spectrophotometry (UV-1700 PharmaSpec UV-Vis spectrophotometer)). It is to be noted that encapsulated drug was left to transform into its degradation products before liposome production and therefore quantified drug is actually TMZ degradation products (MTIC/AIC) and not TMZ. The percentage of TMZ degradation products released at each time was then calculated with the following equation:

$$Drug\ released\ at\ time, T\ (\%) = \frac{Absorbance\ of\ drug\ at\ T}{Absorbance\ of\ maximum\ drug\ in\ dialysed\ membrane}\text{X}\ 100$$

[5]

4. RESULTS AND DISCUSSION

4.1 UV-Vis absorption spectrum for TMZ

The graph below (Figure 12) shows the absorption spectrum for TMZ when dissolved in water (10 µg/mL) at pH 6.3. The absorption peak for TMZ was found to be at 328 nm. Another peak, observed between 255 nm and 266 nm, which is the absorption peak for the active degradation products of TMZ hydrolysis (MTIC and AIC).

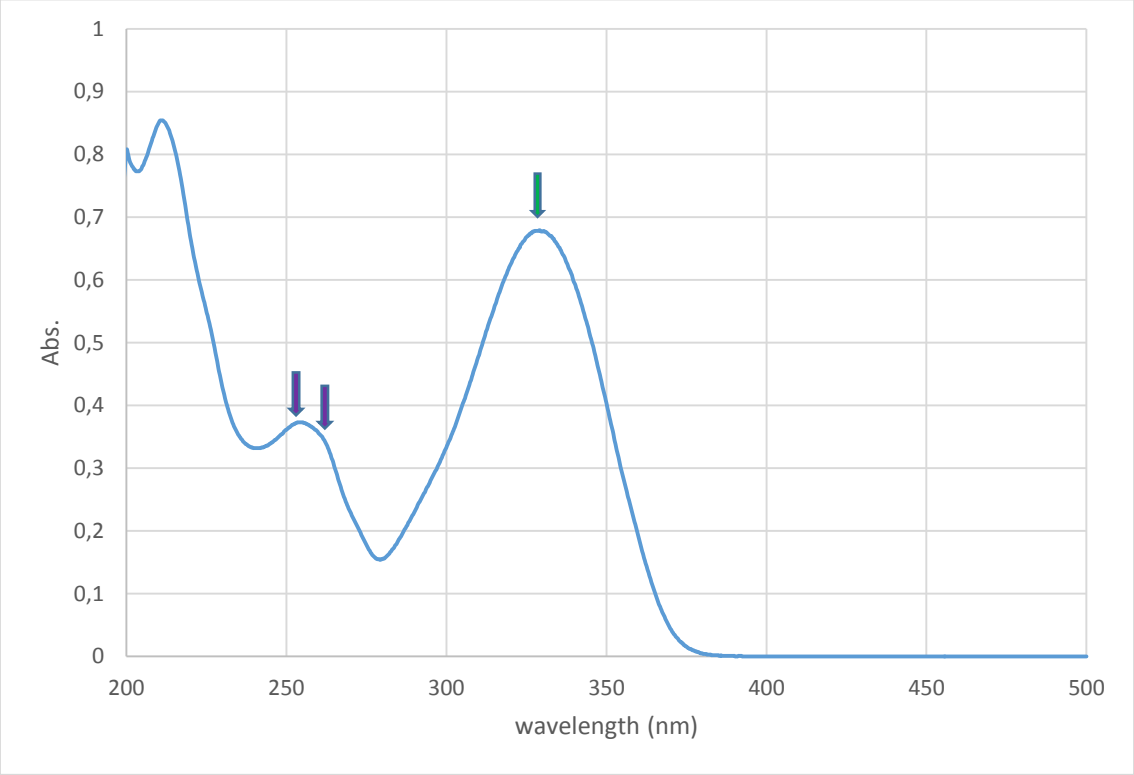

Figure 12: TMZ UV-vis absorption spectrum at pH 6.3

TMZ was dissolved in an array of different solvents: water, acetone, chloroform, ethyl acetate, dichloromethane and dimethyl sulfoxide and concentrations much below their saturation concentration. All UV-vis results showed similar absorption spectra showing that the solvent did not affect TMZ's absorbance.

Although the saturation concentration for TMZ in different solvents varies, TMZ absorbance spectrum was measured at a very low concentration (10 µg/mL), perhaps explaining why the absorbance values do not correlate with the solubility values. However, all showed the characteristic peak around 328 nm showing that these solvents did not alter the TMZ. Results are shown in Table 3.

Table 3: Dissolving TMZ in organic and inorganic solvents

Solvent	Dimethyl Sulfoxide	Dichloromethane	Ethyl Acetate	Chloroform	Acetone	Water
TMZ (µg/ml)	10	10	10	10	10	10
Wavelength (nm)	328.20	328.80	330.40	329.80	328.60	327.80
Abs.	0.170	0.395	0.500	0.355	0.843	0.678
Solubility of TMZ	Soluble 33mg/mL [1], 39mg/mL[2]	Slightly soluble[2]	Very slightly soluble[1]	-	Slightly soluble[1]	Slightly soluble 2-4mg/mL[1], 5mg/mL[2]

4.2 TMZ stability at different pHs and temperatures

TMZ dissolved in PBS (solubility 0.33 mg/mL) at 10 µg/mL uv-spectrum was measured at hourly intervals over 36 hours at 22 °C (Figure 13a) and 37 °C (Figure 13b). The characteristic peak of TMZ at 328 nm (orange) loses its intensity from 0.4 to 0.1 in 10 hours in both cases. And another peak, at 266 nm increases in the same timeframe from around 0.3 to 0.5. We can conclude that at pH 7 at both these temperatures, TMZ is rapidly being converted into its active form over these first 10 hours. Thus the growing peak at 266 m represents the peak for MTIC/AIC.

After acidifying the same solution, concentration 10 µg/mL, to a pH of 5.6 (figure 13c) no significant change was found over a 36 hour period meaning that TMZ does not undergo chemical change to its active alkylating form (MTIC and then AIC) over this time-frame, and is stable.

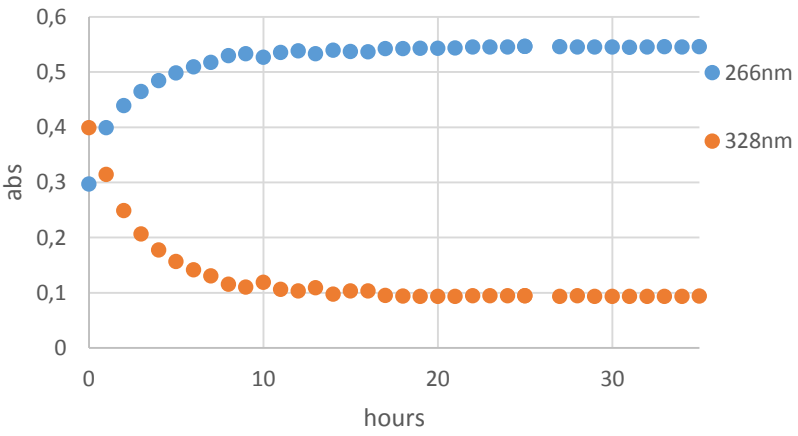

Figure 13a): TMZ stability at 22°C at pH 7 (PBS)

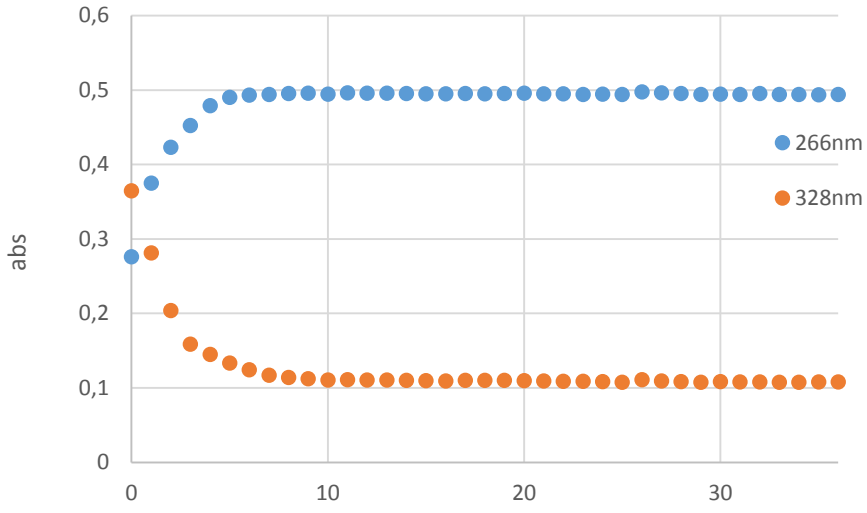

Figure 13b): TMZ stability at 37°C at pH 7 (PBS)

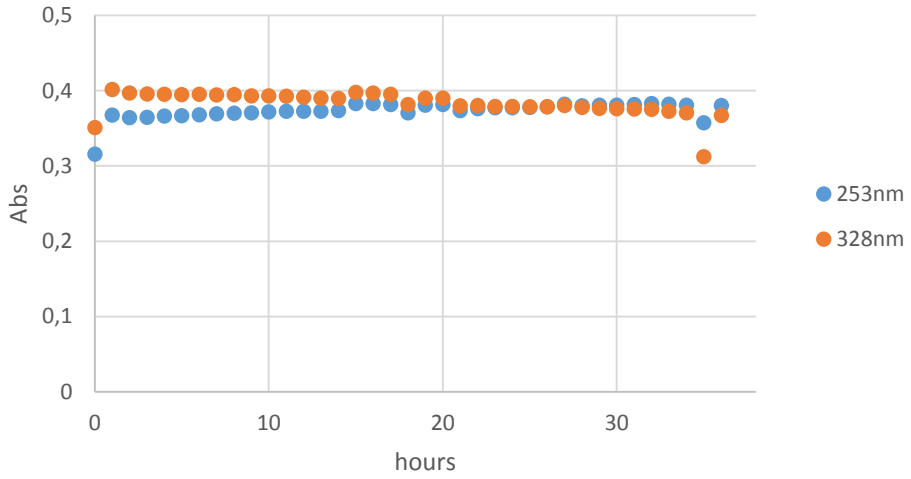

Figure 13c): TMZ stability at 37°C at pH 5.6 (PBS)

Figure 14 shows TMZ at pH 7.2 as well as at increasing pHs, where the characteristic peak for TMZ is present at 328 nm. At pH 11.2 though there is still some TMZ present at 328 nm, the concentration has decreased due to the decrease in absorbance and the quantity of degradation products (around 270) increases drastically. At pH 11.9 and pH 12.3 TMZ has completely degraded as there is no visible peak at 328 nm. This experiment was performed at room temperature (approximately 22 °C). This shows clearly that TMZ is unstable at basic pH and changes conformation immediately after the solution is made basic.

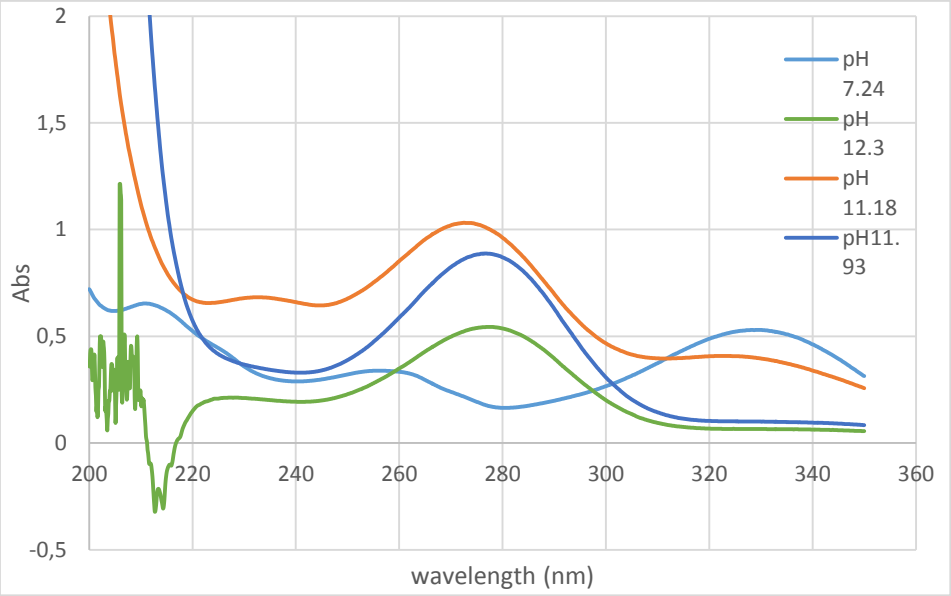

Figure 14: TMZ stability at basic pH

4.3 Liposome Production and Characterization

Figure 15 shows liposomes at 0 hours after production (blue), as well as after 36 hours, liposomes alone (grey). Liposomes were stored at room temperature for 36 hours and re-read through spectroscopy after this time-period. The liposome sample at different time points, showed a very similar UV-vis spectrum curve before and after 36 hours, conferring good stability over this time period under these conditions.

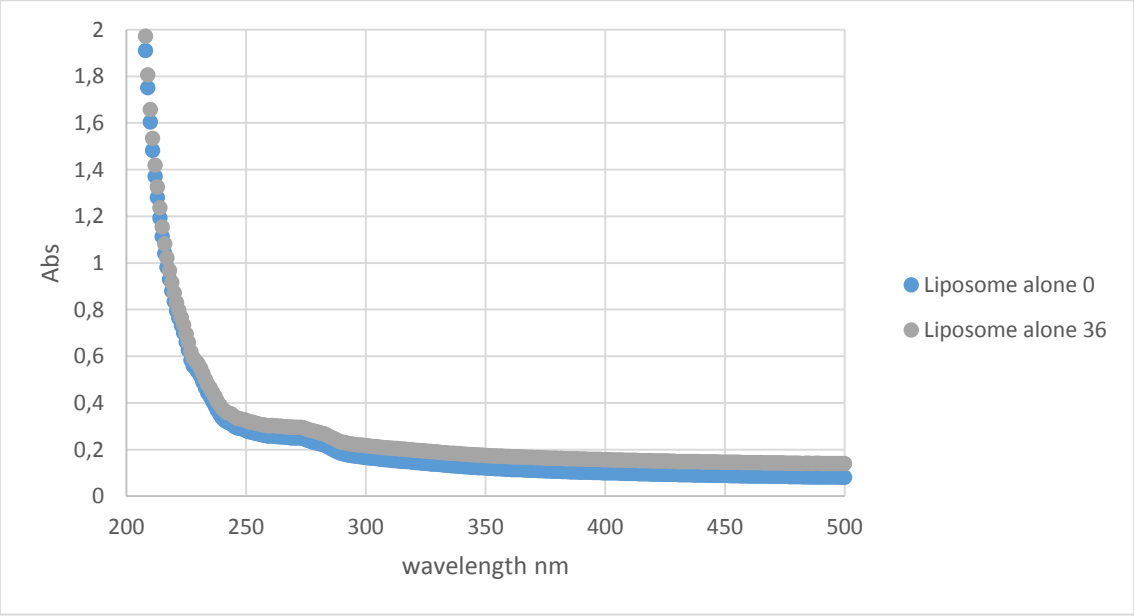

Figure 15: Liposomes after production at hour 0 and 36 hours later.

Table 4 shows liposomes that were produced unloaded (alone) and loaded with TMZ. The size of the liposomes is slightly lower than 200 nm, an ideal size to pass the BBB. The differences in size and in ζ–potential for liposomes and alone and with TMZ were not statistically significant.

Table 4: Size and ζ-potential of TMZ-loaded and unloaded liposomes

	Size (nm)	ζ-potential (mV)
Liposome alone	196±4	-2±2
TMZ-loaded liposome	197±6	-2±1

4.3.1 Liposome Stability at different pH

Due to TMZ decomposition into its degradation products (MTIC/AIC) when the liposomes were being prepared at pH 7.4 in PBS; liposomal size, ζ–potential and PdI were tested as pH of the liposome solution was decreased gradually, to see if the liposomes maintained stability at an acidic pH.

Liposomes showed to maintain a stable size (approximately 200 nm), ζ-potential (close to 0), and a relatively constant PdI (between 0,1 and 0,2) until pH 6. At pH values below this: the average liposome size decreased; the PdI increased significantly to around 0.7, indicative of high polydispersity and therefore a non-uniform liposome size sample; from pH of below 6 zeta-potential started to become significantly more positive. This set of results showed that liposomes appeared to maintain its size, ζ-potential and PdI close to that of liposomes at pH 7.4 (pH of PBS) until it reached a pH of around 6, after which inconsistency was observed.

Liposomes stored since the day of manufacture at pH 6.1 over a 5-day period showed that liposomes did not maintain stability. The size increased from less than 188 nm to over 400 nm, indicating flocculation of the particles. The ZP, and PdI however maintained relative stability. The aggregation of liposomes however is undesirable and thus despite TMZ maintaining stability at this pH, the liposomes do not, meaning that liposomes cannot be produced at pH below 7.

4.3.2 TMZ-Loaded Liposome Production

Figure 16 shows that during liposome production, the characteristic UV-Vis spectrum peak for TMZ is not present (328 nm) whereas the peak for the degradation products, MTIC and AIC (255-266 nm) is. This is because the TMZ solution was previously left to degrade until total degradation so that only one peak as opposed to two appeared, making it easier to quantify. Therefore, quantification was obtained only from the 255-266 nm peak values.

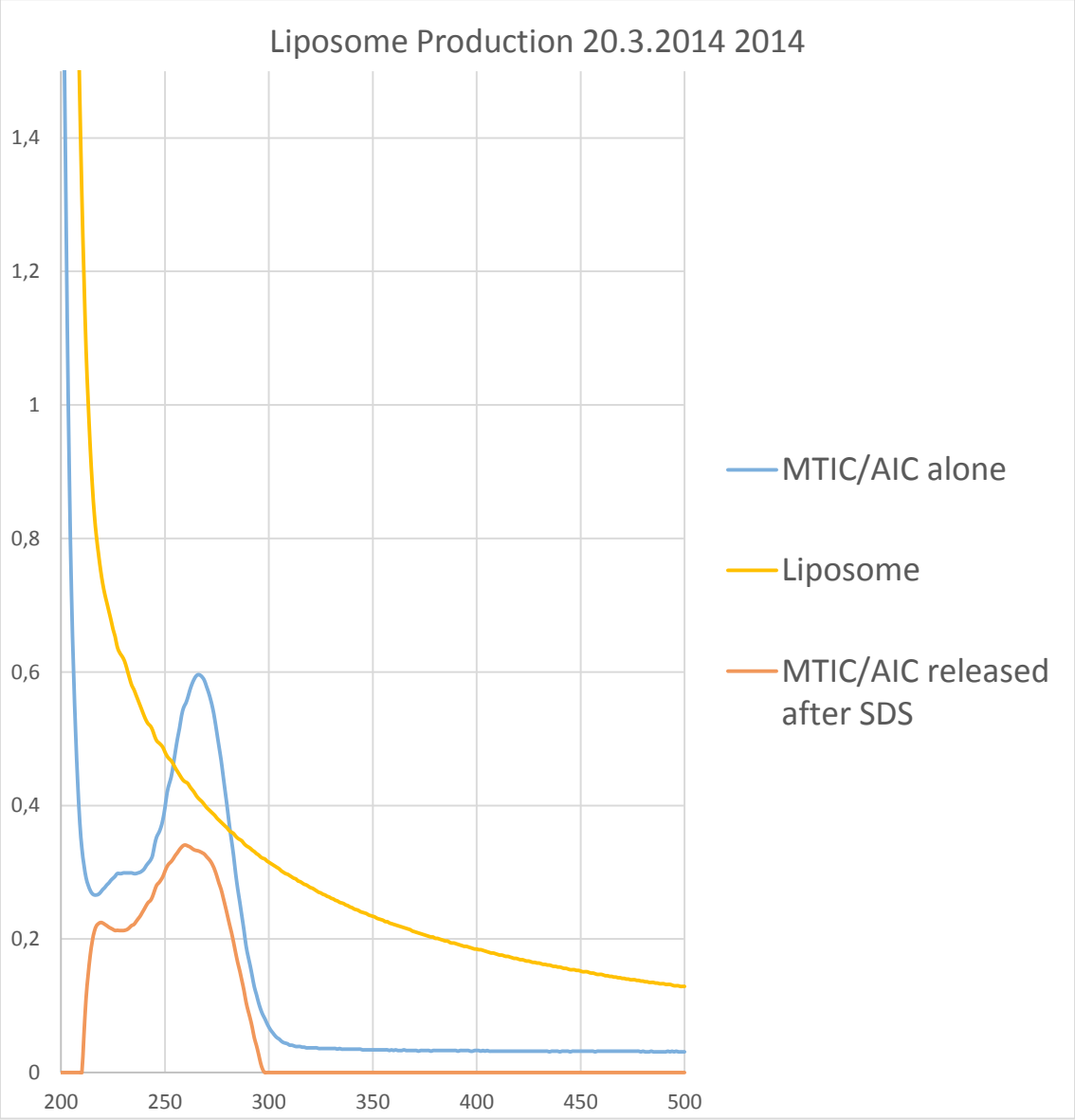

Figure 16: Liposome production: degradation products alone before encapsulation (blue), liposome after being synthesized (yellow), and degradation products released after bursting liposome (red).

TMZ solution alone prior to hydration (blue line), synthesized liposomes (yellow) and drug released after bursting is shown in figure 16. The TMZ quantified upon bursting with sodium dodecyl sulfate (SDS), showed a peak in the characteristic 255-266nm region (dark green line), indicative of drug entrapment. To obtain an approximate concentration of how much drug was present upon bursting of the liposome, another calibration was made for the degradation products alone.

4.3.3 Encapsulation Efficiency of Liposomes NPs

According to the calibration curve of the degradation products of TMZ (Appendix A3), the encapsulation efficiency was calculated and was between 45 and 55%.

4.3.4 Release Study of TMZ-loaded liposomes

Figure 17 shows the results of the release experiments performed on TMZ-loaded liposomes and also with the TMZ alone control. The release experiments were stopped at 51 hours after reaching 50% of the total of TMZ encapsulated in TMZ-loaded liposomes versus the 98% observed for the TMZ solution.

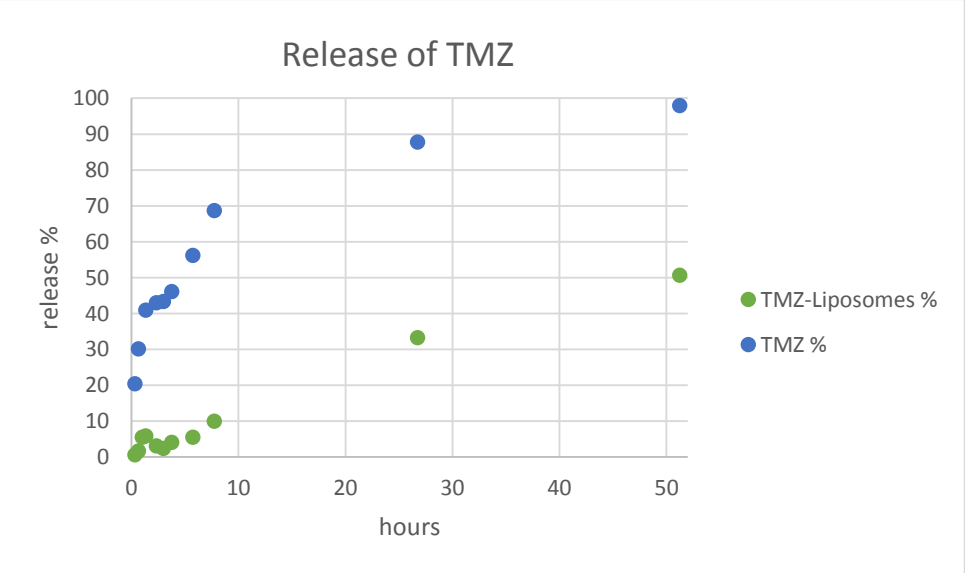

Figure 17: Release of TMZ from TMZ-loaded liposomes (green) and TMZ alone in solution (blue)

These results clearly show that the release in TMZ from liposomes is much slower and sustained compared to the drug alone that has an initial “burst” during the first 10 hours. This is desired property for the nanocarrier being developed as drugs that have a more prolonged release require less frequent drug administration.

4.4 PLGA NP Production and Characterization

Dissolving TMZ (initial mass measured 0.05 mg) in ethyl acetate (EA) to test its stability over time by measuring UV-Vis spectrum over a period of 9 hours. By hour 8 TMZ starts to degrade rapidly (Figure 18).

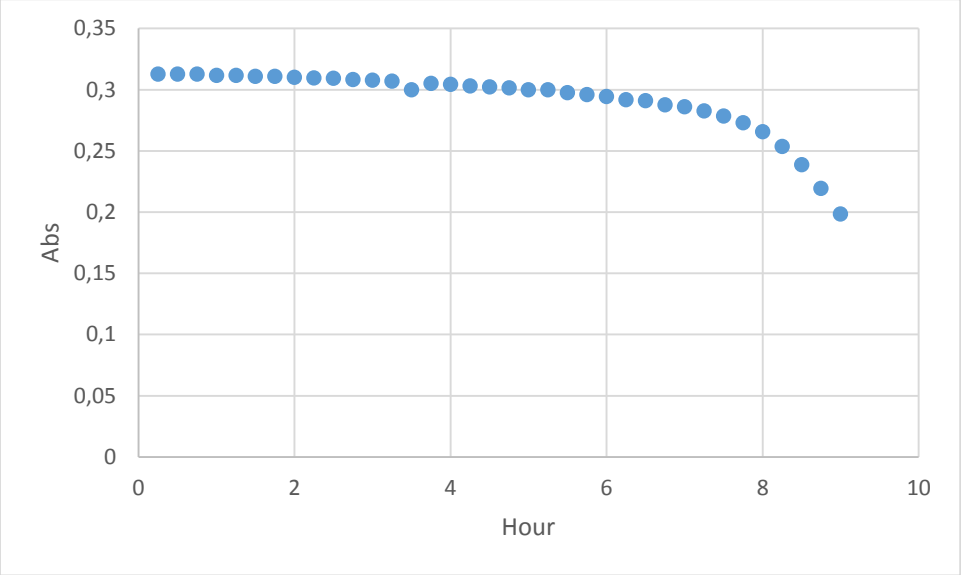

Figure 18: stability of TMZ dissolved in ethyl acetate at 37 °C

The solubility of TMZ in EA is too low to permit use in the experiment; 1mg TMZ failed to dissolve in 2 mL of EA. Therefore subsequent dilutions to obtain desired concentration of 10 µg/mL were required in order to obtain a characteristic UV-vis peak.

As stated previously in the materials and methods chapter an alteration to the conventional protocol of single-emulsion evaporation technique (where organic solvent is only composed of EA) had to be altered because 1 mg of TMZ Is insoluble in 100 µL of EA. The protocol was altered so that 1 mg of TMZ, previously dissolved in 30 µL of DMSO (in which it is highly soluble) was then mixed with 70 µL 0f EA to form an organic phase in this way.

4.4.1 Unloaded PLGA NP Stability over Time

The unloaded PLGA NPs were measured over a period of 14 days to see whether these values maintained, indicating stability of the NPs.

Table 5: Stability of unloaded PLGA NPs over a two week period

	size (nm)	PdI	ZP (mV)
day 1	177± 5	0,08 ± 0,02	-31 ± 3
day 2	176± 4	0,06± 0,03	-31± 2
day 7	179± 4	0,06± 0,03	-31± 3
day 14	183± 6	0,05± 0,03	-29 ± 3

PdI remained under 0.1 showing a good degree of monodisperse sample population and the ZP remained close to -30 mV perhaps explaining how the average size was maintained and the PdI continued below 0.1. A negative ζ-potential shows that this value (demonstrating the electrical potential in the diffuse layer) was negative enough to cause particles to repel each other, thus avoiding flocculation over the two week period over which they were measured.

4.4.2 TMZ-loaded PLGA NPs

Table 6 shows the size, ζ-potential and PdI of the unloaded (PLGA alone) as well as TMZ-loaded PLGA nanoparticles formed through the modified single-emulsion solvent evaporation technique. For the unloaded PLGA NPs, the size at 177 nm is a good size as it is small enough to eventually cross the BBB. The PdI is below 0.1 showing that it is considered a mono-disperse sample of PLGA nanoparticles. The zeta-potential, at -31 mV shows potential stability and a reduced possibility of flocculation occurring. With the TMZ-loaded PLGA particles, the size was similar to that of PLGA alone (176 nm), and PdI around 0.1 are good indicators as above. However in contrast, the ζ-potential decreased to -2 mV, confirming the encapsulation of TMZ.

However, one can note that the ZP is very close to zero compared to the ZP of the unloaded PLGA nanoparticles (where ZP was approximately -30 mV). This can be due to TMZ being adsorbed at the surface of the nanoparticles, causing the charge to become more positive.

Table6: Size, zeta-potential and polydispersity of alone (unloaded) and TMZ-loaded PLGA nanoparticles

NP	**PLGA alone**	**TMZ-loaded PLGA**
Size (nm)	177 ± 5	176 ± 7
ζ-potential (mV)	-31 ± 3	-2 ± 4
PdI	0,08 ± 0,02	0,11 ± 0,03

The resulting supernatant collected upon centrifugation was diluted 10x and measured in order to get an approximation of the EE% according to the calibration curve presented in appendix A1.

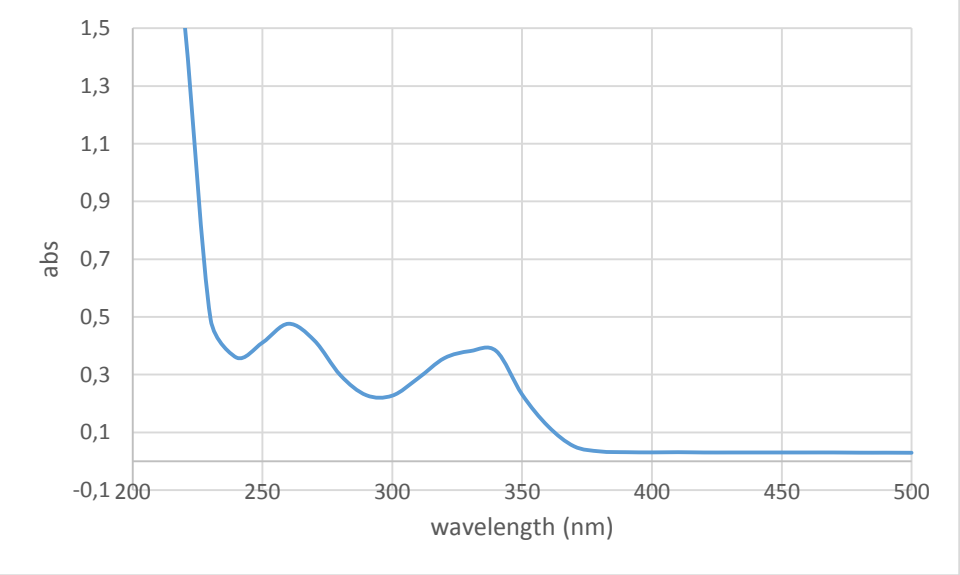

Figure 19: TMZ-loaded PLGA NP supernatant UV-Vis spectrum

Figure 19 shows the TMZ and its respective degradation products that were present in the supernatant upon centrifugation of the prepared nanoparticles. The solution was diluted 10x to obtain a quantifiable spectrophotometric analysis (where absorption peak is below 1).

For calculating the encapsulation efficiency (EE%), one must do indirectly by measuring how much was not encapsulated, i.e. what remained in the supernatant after centrifugation of the resulting NP pellet.

The EE% was approximately 84% according to the calibration curve for TMZ and its degradation products (Appendix A1).

4.4.3 TMZ-Loaded PLGA NP Stability over Time

Results from performing Dynamic Light Scattering and Laser Doppler Velocimetry are presented in Table 7. One can see that the size of the TMZ-loaded nanoparticles increased more than four-fold in a four day period indicating NP aggregation. This is most probably due to the low ZP (-3.66 and -3.90) compared to the unloaded PLGA particles that had a zeta potential of around -30 mV which correlated with unloaded PLGA particles maintaining their size. Therefore one can conclude that this technique was not successful in producing stable TMZ-loaded nanoparticles.

Firstly, it is highly likely that the NPs did not contain TMZ. And that the TMZ molecules must have coated the surface, causing the decrease in ZP. A hypothesis for little or no entrapment is that TMZ may have remained in the aqueous phase. The TMZ although dissolved before-hand in DMSO, was then added to ethyl acetate (In which It is very poorly soluble); and this organic phase was then added to the aqueous phase, to which TMZ may have had much more affinity. Therefore when the organic phase was evaporated the TMZ was probably not entrapped in the PLGA droplets but spread out in the aqueous phase. Hence, the TMZ in the aqueous phase may have adsorbed onto the nanoparticle surface only after PLGA NP production was complete (upon filtration and stabilization overnight at 4 °C).

Table 7: Stability of TMZ-loaded PLGA NPs

PLGA- TMZ	**size (nm)**	**ZP (mV)**	**PdI**
Day 1	176 ± 6	-4 ± 1	0.05 ± 0,02
Day 4	813 ± 8	-4 ± 3	0.10 ± 0,04

4.4.4 Modification of PLGA NP Production Method

TMZ-PLGA NPs produced with polysorbate 80

The TMZ-loaded PLGA nanoparticles produced after modifying the supernatant from pluronic f127 to polysorbate 80 in an attempt to produce more stable particles, produced the results shown in table 8.

Table 8: TMZ-loaded NPs produced with Polysorbate 80 over time

	Size(nm)	ζ-potential (mV)	PdI
day 1	133 ± 6	5± 2	0,09±0,01
day 2	132± 5	0± 1	0.15±0.02
day 3	119± 6	0± 1	0.25±0.03
day 4	117± 4	0± 1	0.21±0.03

The polydispersity increases from 0.09 to 0.25 in 3 days, indicating that the NPs size in the sample are too polydisperse (> 0.1), also explaining the change in average size of the nanoparticles. The zeta potential also decreases. As all the parameters vary substantially, one can conclude that the particles produced through single emulsion solvent evaporation technique using polysorbate 80 instead of pluronic f127, are not stable and the NPs must be produced by a different procedure.

TMZ-PLGA NPs produced at half PLGA/TMZ loading percentage

TMZ-loaded PLGA particles produced with 0.5 mg instead of 1 mg as used in the previous experiments and as described in the initial protocol for producing PLGA NPs through the single solvent emulsion evaporation technique.

Table9: TMZ-loaded NPs produced with 5% TMZ (0.5mg)

	Size (nm)	ζ-potential (mV)	PdI
TMZ/PLGA (5%)	168± 4	-1± 1	0.45±0.03

The results in Table 9 show that the aqueous phase used was PBS again and the mass of TMZ was 0.5 mg. The polydispersity of the sample was too high (>0,1) and the ζ-potential is very close to 0 indicating yet again that TMZ has been adsorbed on the surface and has not been encapsulated. If it had been encapsulated, one would expect a zeta potential close to that of the unloaded PLGA NPs that have a ZP of around -30 mV when pluronic f127 is used as the stabilizer. The results also show a very high polysdispersion (>0.1), an additional factor that makes this method unsuitable.

5. CONCLUSIONS AND FUTURE PERSPECTIVES

This project allowed for a detailed understanding of the behaviour and physichochemical properties of TMZ; a drug that is used in wide-scale as an adjuvant chemotherapeutic agent. Encapsulating this drug, by developing a nanocarrier, to reduce systemic side-effects and increase its bioavailability was the main aim of this project.

As confirmed by the experiments carried out, TMZ is amphiphilic. Although successful in developing PLGA particles alone, through single solvent emulsion evaporation technique, encapsulation of TMZ was not successful in PLGA NPs. As the TMZ molecule is not entirely hydrophobic, failure to form PLGA/TMZ droplets -as the organic phase evaporated- may have resulted as a consequence of affinity of the compound for the aqueous phase. Further work should be carried out using the double-emulsion solvent evaporation technique a method that has been developed for encapsulation of hydrophilic molecules.

Despite the difficulties in encapsulating TMZ in PLGA, encapsulation in liposomes was successful with an encapsulation efficiency of approximately 45-50%, observed upon directly bursting the liposomes and measuring the TMZ released. These results are promising, as well as novel, as there is no literature reporting TMZ encapsulated in liposomes.

Future perspectives are to test the efficacy of these TMZ-loaded liposomes by testing their cytotoxicity in glioma cell lines (U87 cell lines) and compare these results to cytotoxicity of TMZ alone. Once the efficiency of these liposomes are tested in cells, functionalization with ligands specific to allow these NPs to cross the BBB and bind to cells in the brain parenchyma would have to be carried out in order to enable the drug to reach its target. To enhance the cytotoxicity provided by TMZ, direct inhibitors of DNA-repair enzymes (such as poly (ADP-ribose) polymerase, PARP inhibitor, could be encapsulated along with TMZ.

Another important barrier to take into consideration in treatment of GBM with TMZ, is the high resistance to therapy seen in approximately 60% of patients, due to non-methylation of the MGMT gene, the DNA repair enzyme which interferes with the alkylation caused by TMZ. A way to circumvent this problem would be to use MGMT-specific siRNA- loaded liposomes, functionalized specifically towards the tumour astrocytic cells, in order to block the MGMT gene, and thus prevent such high levels of resistance to TMZ chemotherapy.

It can be therefore concluded that this dissertation project presents findings that will serve as the foundation for future work in the treatment of this specific disease through NP DDS.

6. REFERENCES

1. Danhier, F. *et al.* PLGA-based nanoparticles: An overview of biomedical applications. *J. Control. Release* **161,** 505–522 (2012).

2. Louis, D. N. *et al.* The 2007 WHO Classification of Tumours of the Central Nervous System. *Acta Neuropathol.* **114,** 97–109 (2007).

3. Esiri, M. & Oppenheimer, D. *Diagnostic neuropathology*. 426–446 (Blackwell Scientific Publications, 1989).

4. Patel, T., Zhou, J., Piepmeier, J. M. & Saltzman, W. M. Polymeric nanoparticles for drug delivery to the central nervous system. *Adv. Drug Deliv. Rev.* **64,** 701–705 (2012).

5. Stupp, R. *et al.* Radiotherapy plus concomitant and adjuvant temozolomide for glioblastoma. *N. Engl. J. Med.* **352,** 987–96 (2005).

6. Friedman, H. S., Kerby, T. & Calvert, H. Temozolomide and Treatment of Malignant Glioma Temozolomide and Treatment of Malignant Glioma 1. 2585–2597 (2000).

7. Chamberlain, M. C. Temozolomide: therapeutic limitations in the treatment of adult high-grade gliomas. *Expert Rev. Neurother.* **10,** 1537–1544 (2010).

8. Andrasi, M., Bustos, R., Gaspar, A., Gomez, F. a & Klekner, A. Analysis and stability study of temozolomide using capillary electrophoresis. *J. Chromatogr. B. Analyt. Technol. Biomed. Life Sci.* **878,** 1801–8 (2010).

9. Ekeblad, S. *et al.* Temozolomide as monotherapy is effective in treatment of advanced malignant neuroendocrine tumors. *Clin. Cancer Res.* **13,** 2986–2991 (2007).

10. Ricard, D. *et al.* Dynamic history of low-grade gliomas before and after temozolomide treatment. *Ann. Neurol.* **61,** 484–490 (2007).

11. Middleton, M. R. *et al. Randomized phase III study of temozolomide versus dacarbazine in the treatment of patients with advanced metastatic malignant melanoma. J. Clin. Oncol.* **18,** 158–166 (2000).

12. Raverot, G. *et al.* Temozolomide treatment in aggressive pituitary tumors and pituitary carcinomas: a French multicenter experience. *J. Clin. Endocrinol. Metab.* **95,** 4592–4599 (2010).

13. PubChem. Temozolomide. *Natl. Cent. Biotechnol. Inf.* (2013). at <http://pubchem.ncbi.nlm.nih.gov/summary/summary.cgi?cid=5394#x94>

14. Temodar Capsules (Schering). (2007). at <http://www.theodora.com/drugs/temodar_capsules_schering.html>

15. Ibrahim, S. *Clinical pharmacology/biopharmaceutics review: Temozolomide*. 1–29 (1998). at <http://www.accessdata.fda.gov/drugsatfda_docs/nda/99/21029_Temodar_clinphrmr.pdf>

16. Heywood, R. M. *et al.* Enhanced stability and activity of temozolomide in primary glioblastoma multiforme cells with cucurbit[n]uril. *Chem. Commun.* **48,** 9843 (2012).

17. Patil, R. *et al.* Temozolomide delivery to tumor cells by a multifunctional nano vehicle based on poly(β-L-malic acid). *Pharm. Res.* **27,** 2317–2329 (2010).

18. Tian, X.-H. *et al.* Enhanced brain targeting of temozolomide in polysorbate-80 coated polybutylcyanoacrylate nanoparticles. *Int. J. Nanomedicine* **6,** 445–52 (2011).

19. Wesolowski, J. R., Rajdev, P. & Mukherji, S. K. Temozolomide (Temodar). *Ajnr Am. J. Neuroradiol.* **5,** 37–38 (2010).

20. EMEA. *Temodal: EPAR Scientific Discussion*. (1994). at <http://www.ema.europa.eu/docs/en_GB/document_library/EPAR_-_Scientific_Discussion/human/000229/WC500035617.pdf>

21. AHMP. *Temozolomide SUN CHMP assessment report EMA/CHMP/197697/2011*. 1–20 (2011). at <http://www.ema.europa.eu/docs/en_GB/document_library/EPAR_-_Public_assessment_report/human/002198/WC500109707.pdf>

22. Immordino, M. L., Dosio, F. & Cattel, L. Stealth liposomes: review of the basic science, rationale, and clinical applications, existing and potential. *Int. J. Nanomedicine* **1,** 297–315 (2006).

23. Lanz-landázuri, A. & et al. Poly(methyl malate) Nanoparticles: Formation, Degradation, and Encapsulation of Anticancer Drugs. *Macromol Biosci.* **11,** 1370–1377 (2011).

24. Stevanovi, M. & Uskokovi, D. Poly(lactide-co-glycolide)-based Micro and Nanoparticles for the Controlled Drug Delivery of Vitamins. *Curr. Nanosci.* **5,** 1573–4137 (2009).

25. Singh, M., Gulati, M., Singh, S. & Grover, M. Lipophilic drug derivatives in liposomes. *Int. J. Pharm.* **165,** 129–168 (1998).

26. Mishra, G. P., Bagui, M., Tamboli, V. & Mitra, A. K. Recent applications of liposomes in ophthalmic drug delivery. *J. Drug Deliv.* **2011,** 863734 (2011).

27. Caraglia, M. *et al.* Phase II study of temozolomide plus pegylated liposomal doxorubicin in the treatment of brain metastases from solid tumours. *Cancer Chemother. Pharmacol.* **57,** 34–9 (2006).

28. Kato, T. *et al.* Efficient delivery of liposome-mediated MGMT-siRNA reinforces the cytotoxity of temozolomide in GBM-initiating cells. *Gene Ther.* **17,** 1363–1371 (2010).

29. Dijkstra, J., van Galen, M., Regts, D. & Scherphof, G. Uptake and processing of liposomal phospholipids by Kupffer cells in vitro. *Eur. J. Biochem.* **148,** 391–397 (1985).

30. Koning, G. A., Morselt, H. W., Kamps, J. A. & Scherphof, G. L. Uptake and intracellular processing of PEG-liposomes and PEG-immunoliposomes by kupffer cells in vitro 1 *. *J. Liposome Res.* **11,** 195–209 (2001).

31. Basu, M. K. & Lala, S. Macrophage specific drug delivery in experimental leishmaniasis. *Curr. Mol. Med.* **4,** 681–689 (2004).

32. Yan, X., Scherphof, G. L. & Kamps, J. A. A. M. Liposome opsonization. *J. Liposome Res.* **15,** 109–139 (2005).

33. Harashima, H., Sakata, K., Funato, K. & Kiwada, H. Enhanced hepatic uptake of liposomes through complement activation depending on the size of liposomes. *Pharm. Res.* **11,** 402–406 (1994).

34. Oja, C. D., Semple, S. C., Chonn, A. & Cullis, P. R. Influence of dose on liposome clearance: critical role of blood proteins. *Biochim. Biophys. Acta* **1281,** 31–37 (1996).

35. Chonn, A., Semple, S. C. & Cullis, P. R. Association of blood proteins with large unilamellar liposomes in vivo. Relation to circulation lifetimes. *J. Biol. Chem.* **267,** 18759–18765 (1992).

36. Damen, J. Transfer and exchange of phospholipid between small unilamellar liposomes and rat plasma high-density lipoproteins: dependence on cholesterol and phospholipid composition. *Biochim Biophys Acta* **665,** 538–45 (2005).

37. Senior, J. Is half-life of circulating liposomes determined by changes in their permeability? . *FEBS Lett* **145,** 109–14 (1982).

38. Park, Y. S., Maruyama, K. & Huang, L. Some negatively charged phospholipid derivatives prolong the liposome circulation in vivo. *Biochim. Biophys. Acta* **1108,** 257–260 (1992).

39. Nishikawa, K., Arai, H. & Inoue, K. Scavenger receptor-mediated uptake and metabolism of lipid vesicles containing acidic phospholipids by mouse peritoneal macrophages. *J. Biol. Chem.* **265,** 5226–5231 (1990).

40. Chonn, A., Cullis, P. R. & Devine, D. V. The role of surface charge in the activation of the classical and alternative pathways of complement by liposomes. *J. Immunol.* **146,** 4234–4241 (1991).

41. Torchilin, V. P. Liposomes as targetable drug carriers. *Crit. Rev. Ther. Drug Carrier Syst.* **2,** 65–115 (1985).

42. Torchilin, V. P. Recent advances with liposomes as pharmaceutical carriers. *Nat. Rev. Drug Discov.* **4,** 145–160 (2005).

43. Blume, G. & Cevc, G. Molecular mechanism of the lipid vesicle longevity in vivo. *Biochim. Biophys. Acta* **1146,** 157–168 (1993).

44. Klibanov, A. L., Maruyama, K., Torchilin, V. P. & Huang, L. Amphipathic polyethyleneglycols effectively prolong the circulation time of liposomes. *FEBS Lett.* **268,** 235–237 (1990).

45. Torchilin, V. P. *et al.* Poly(ethylene glycol) on the liposome surface: on the mechanism of polymer-coated liposome longevity. *Biochim. Biophys. Acta* **1195,** 11–20 (1994).

46. Moghimi, S. M. & Szebeni, J. Stealth liposomes and long circulating nanoparticles: critical issues in pharmacokinetics, opsonization and protein-binding properties. *Prog. Lipid Res.* **42,** 463–478 (2003).

47. Pan, X. Q., Wang, H. & Lee, R. J. Antitumor activity of folate receptor-targeted liposomal doxorubicin in a KB oral carcinoma murine xenograft model. *Pharm. Res.* **20,** 417–422 (2003).

48. Reddy, J. A. *et al.* Folate-targeted, cationic liposome-mediated gene transfer into disseminated peritoneal tumors. *Gene Ther.* **9,** 1542–1550 (2002).

49. Leamon, C. P., Cooper, S. R. & Hardee, G. E. Folate-liposome-mediated antisense oligodeoxynucleotide targeting to cancer cells: evaluation in vitro and in vivo. *Bioconjug. Chem.* **14,** 738–47 (2003).

50. Eavarone, D. A., Yu, X. & Bellamkonda, R. V. Targeted drug delivery to C6 glioma by transferrin-coupled liposomes. *J. Biomed. Mater. Res.* **51,** 10–14 (2000).

51. Immordino, M. L. & Cattel, L. Stealth liposomes : review of the basic science , rationale , and clinical applications , existing and potential. 297–315 (2006).

52. Peer, D. & Margalit, R. Loading mitomycin C inside long circulating hyaluronan targeted nano-liposomes increases its antitumor activity in three mice tumor models. *Int. J. Cancer* **108,** 780–789 (2004).

53. Rogers, J. A. & Anderson, K. E. The potential of liposomes in oral drug delivery. *Crit. Rev. Ther. Drug Carrier Syst.* **15,** 421–480 (1998).

54. Van Winden EC. Freeze-drying of liposomes: theory and practice. *Methods Enzym.* **367,** 99–110 (2003).

55. Knight, V., Koshkina, N. V, Golunski, E., Roberts, L. E. & Gilbert, B. E. Cyclosporin A aerosol improves the anticancer effect of paclitaxel aerosol in mice. *Trans. Am. Clin. Climatol. Assoc.* **115,** 395–404; discussion 404 (2004).

56. Vyas, S. P. & Khatri, K. Liposome-based drug delivery to alveolar macrophages. *Expert Opin. Drug Deliv.* **4,** 95–99 (2007).

57. Leung , K. The stability of liposomes to ultrasonic nebulisation. *Int. J. Pharm.* **145,** 95–102 (1996).

58. Venkataraman, C., Chattopadhyay, S., Bellare, J. & Ehrman, S. H. Morphology and bilayer integrity of small liposomes during aerosol generation by air-jet nebulisation. *J. Nanoparticle Res.* **14,** (2012).

59. El Maghraby, G. M. M., Williams, A. C. & Barry, B. W. Can drug-bearing liposomes penetrate intact skin? *J. Pharm. Pharmacol.* **58,** 415–429 (2006).

60. Frisbie, D. D., McIlwraith, C. W., Kawcak, C. E., Werpy, N. M. & Pearce, G. L. Evaluation of topically administered diclofenac liposomal cream for treatment of horses with experimentally induced osteoarthritis. *Am. J. Vet. Res.* **70,** 210–215 (2009).

61. Vutla, N. B., Betageri, G. V & Banga, A. K. Transdermal iontophoretic delivery of enkephalin formulated in liposomes. *J. Pharm. Sci.* **85,** 5–8 (1996).

62. Goldberg, S. N. *et al.* Percutaneous tumor ablation: increased necrosis with combined radio-frequency ablation and intravenous liposomal doxorubicin in a rat breast tumor model. *Radiology* **222,** 797–804 (2002).

63. Oussoren, C. & Storm, G. Liposomes to target the lymphatics by subcutaneous administration. *Adv. Drug Deliv. Rev.* **50,** 143–156 (2001).

64. Phillips, W. T., Klipper, R. & Goins, B. Novel method of greatly enhanced delivery of liposomes to lymph nodes. *J. Pharmacol. Exp. Ther.* **295,** 309–313 (2000).

65. Song, G., Wu, H., Yoshino, K. & Zamboni, W. C. Factors affecting the pharmacokinetics and pharmacodynamics of liposomal drugs. *J. Liposome Res.* **22,** 177–192 (2012).

66. Moser, C., Amacker, M. & Zurbriggen, R. Influenza virosomes as a vaccine adjuvant and carrier system. *Expert Rev. Vaccines* **10,** 437–446 (2011).

67. Bungener, L., Huckriede, A., Wilschut, J. & Daemen, T. Delivery of protein antigens to the immune system by fusion-active virosomes: a comparison with liposomes and ISCOMs. *Biosci. Rep.* **22,** 323–338 (2002).

68. Bungener, L. *et al.* Virosome-mediated delivery of protein antigens to dendritic cells. *Vaccine* **20,** 2287–2295 (2002).

69. Nobuto, H. *et al.* Evaluation of systemic chemotherapy with magnetic liposomal doxorubicin and a dipole external electromagnet. *Int. J. Cancer* **109,** 627–635 (2004).

70. Khaw, B. A., Torchilin, V. P., Vural, I. & Narula, J. Plug and seal: prevention of hypoxic cardiocyte death by sealing membrane lesions with antimyosin-liposomes. *Nat. Med.* **1,** 1195–1198 (1995).

71. Centisa, V., Proulxc, P. & Vermettea, P. PEGylated liposomes encapsulating human hemoglobin enhance oxygen transfer and cell proliferation while decreasing cell hypoxia in fibrin. *Biochem. Eng. J.* **55,** 162–168 (2011).

72. Konno, H., Matin, A. F., Maruo, Y., Nakamura, S. & Baba, S. Liposomal ATP protects the liver from injury during shock. *Eur. Surg. Res.* **28,** 140–145 (1996).

73. Laham, A. *et al.* Liposomally entrapped adenosine triphosphate. Improved efficiency against experimental brain ischaemia in the rat. *J. Chromatogr.* **440,** 455–458 (1988).

74. Derycke, A. S. L. & de Witte, P. A. M. Liposomes for photodynamic therapy. *Adv. Drug Deliv. Rev.* **56,** 17–30 (2004).

75. Makadia, H. K. & Siegel, S. J. Poly Lactic-co-Glycolic Acid (PLGA) as Biodegradable Controlled Drug Delivery Carrier. *Polymers (Basel).* **3,** 1377–1397 (2011).

76. Kumari, A., Yadav, S. K. & Yadav, S. C. Biodegradable polymeric nanoparticles based drug delivery systems. *Colloids Surfaces B Biointerfaces* **75,** 1–18 (2010).

77. Frank, A., Rath, S. K. & Venkatraman, S. S. Controlled release from bioerodible polymers: Effect of drug type and polymer composition. *J. Control. Release* **102,** 333–344 (2005).

78. Eniola, A. O., Rodgers, S. D. & Hammer, D. A. Characterization of biodegradable drug delivery vehicles with the adhesive properties of leukocytes. *Biomaterials* **23,** 2167–2177 (2002).

79. Holy, C. E., Dang, S. M., Davies, J. E. & Shoichet, M. S. In vitro degradation of a novel poly(lactide-co-glycolide) 75/25 foam. *Biomaterials* **20,** 1177–1185 (1999).

80. Cai, Q., Shi, G., Bei, J. & Wang, S. Enzymatic degradation behavior and mechanism of Poly(lactide-co-glycolide) foams by trypsin. *Biomaterials* **24,** 629–638 (2003).

81. Li, S., Girard, A., Garreau, H. & Vert, M. Enzymatic degradation of polylactide stereocopolymers with predominant D-lactyl contents. *Polym. Degrad. Stab.* **71,** 61–67 (2000).

82. Taluja, A., Youn, Y. S. & Bae, Y. H. Novel approaches in microparticulate PLGA delivery systems encapsulating proteins. *J. Mater. Chem.* **17,** 4002 (2007).

83. Okada, H. & Toguchi, H. Biodegradable microspheres in drug delivery. *Crit. Rev. Ther. Drug Carrier Syst.* **12,** 1–99 (1995).

84. Panyam, J., Zhou, W.-Z., Prabha, S., Sahoo, S. K. & Labhasetwar, V. Rapid endo-lysosomal escape of poly(DL-lactide-co-glycolide) nanoparticles: implications for drug and gene delivery. *FASEB J.* **16,** 1217–1226 (2002).

85. Acharya, S. & Sahoo, S. K. PLGA nanoparticles containing various anticancer agents and tumour delivery by EPR effect. *Adv. Drug Deliv. Rev.* **63,** 170–183 (2011).

86. Arshady, R. Preparation of biodegradable microspheres and microcapsules: 2. Polyactides and related polyesters. *J. Control. Release* **17,** 1–21 (1991).

87. Vasir, J. K. & Labhasetwar, V. Biodegradable nanoparticles for cytosolic delivery of therapeutics. *Adv. Drug Deliv. Rev.* **59,** 718–728 (2007).

88. Hans, M. L. & Lowman, A. M. Biodegradable nanoparticles for drug delivery and targeting. *Curr. Opin. Solid State Mater. Sci.* **6,** 319–327 (2002).

89. Sahoo, S. K., Panyam, J., Prabha, S. & Labhasetwar, V. Residual polyvinyl alcohol associated with poly (D,L-lactide-co-glycolide) nanoparticles affects their physical properties and cellular uptake. *J. Control. Release* **82,** 105–114 (2002).

90. Hornig, S., Heinze, T., Becerbc, R. & Schubert, U. Synthetic polymeric nanoparticles by nanoprecipitation. *J. Mater. Chem.* **19,** 3838–3840 (2009).

91. Sahoo, S. K. & Labhasetwar, V. Nanotech approaches to drug delivery and imaging. *Drug Discov. Today* **8,** 1112–1120 (2003).

92. Sahoo, S. K., Dilnawaz, F. & Krishnakumar, S. Nanotechnology in ocular drug delivery. *Drug Discov. Today* **13,** 144–151 (2008).

93. Chittasupho, C. *et al.* ICAM-1 targeting of doxorubicin-loaded PLGA nanoparticles to lung epithelial cells. *Eur. J. Pharm. Sci.* **37,** 141–150 (2009).

94. Xie, J. & Wang, C.-H. Self-assembled biodegradable nanoparticles developed by direct dialysis for the delivery of paclitaxel. *Pharm. Res.* **22,** 2079–2090 (2005).

95. Guo, J. *et al.* Aptamer-functionalized PEG-PLGA nanoparticles for enhanced anti-glioma drug delivery. *Biomaterials* **32,** 8010–8020 (2011).

96. Danhier, F. *et al.* Targeting of tumor endothelium by RGD-grafted PLGA-nanoparticles. *Methods Enzymol.* **508,** 157–175 (2012).

97. Betancourt, T., Brown, B. & Brannon-Peppas, L. Doxorubicin-loaded PLGA nanoparticles by nanoprecipitation: preparation, characterization and in vitro evaluation. *Nanomedicine (Lond).* **2,** 219–232 (2007).

98. Yoo, H. S., Oh, J. E., Lee, K. H. & Park, T. G. Biodegradable nanoparticles containing doxorubicin-PLGA conjugate for sustained release. *Pharm. Res.* **16,** 1114–1118 (1999).

99. Park, H. *et al.* Multifunctional nanoparticles for combined doxorubicin and photothermal treatments. *ACS Nano* **3,** 2919–2926 (2009).

100. Liang, C. *et al.* Improved therapeutic effect of folate-decorated PLGA-PEG nanoparticles for endometrial carcinoma. *Bioorganic Med. Chem.* **19,** 4057–4066 (2011).

101. Zhang, Z., Huey Lee, S. & Feng, S. S. Folate-decorated poly(lactide-co-glycolide)-vitamin E TPGS nanoparticles for targeted drug delivery. *Biomaterials* **28,** 1889–1899 (2007).

102. Gómez-Gaete, C., Tsapis, N., Besnard, M., Bochot, A. & Fattal, E. Encapsulation of dexamethasone into biodegradable polymeric nanoparticles. *Int. J. Pharm.* **331,** 153–159 (2007).

103. Reddy, M. K., Wu, L., Kou, W., Ghorpade, A. & Labhasetwar, V. Superoxide dismutase-loaded PLGA nanoparticles protect cultured human neurons under oxidative stress. *Appl. Biochem. Biotechnol.* **151,** 565–577 (2008).

104. Hu, K. *et al.* Lactoferrin conjugated PEG-PLGA nanoparticles for brain delivery: Preparation, characterization and efficacy in Parkinsons disease. *Int. J. Pharm.* **415,** 273–283 (2011).

105. Bondioli, L. *et al.* PLGA nanoparticles surface decorated with the sialic acid, N-acetylneuraminic acid. *Biomaterials* **31,** 3395–3403 (2010).

106. Tosi, G. *et al.* Targeting the central nervous system: In vivo experiments with peptide-derivatized nanoparticles loaded with Loperamide and Rhodamine-123. *J. Control. Release* **122,** 1–9 (2007).

107. Tosi, G. *et al.* Sialic acid and glycopeptides conjugated PLGA nanoparticles for central nervous system targeting: In vivo pharmacological evidence and biodistribution. *J. Control. Release* **145,** 49–57 (2010).

108. Zhang, D. *et al.* The Effect of Temozolomide/Poly(lactide-co-glycolide) (PLGA)/Nano-Hydroxyapatite Microspheres on Glioma U87 Cells Behavior. *Int. J. Mol. Sci.* **13,** 1109–25 (2012).

109. Zhang, H. & Gao, Z. Temozolomide/PLGA microparticles and antitumor activity against Glioma C6 cancer cells in vitr. *Int. J. Pharm.* **329,** 122–128 (2007).

110. Jain, D. *et al.* Unraveling the cytotoxic potential of Temozolomide loaded into PLGA nanoparticles. *DARU J. Pharm. Sci.* **22,** 1–9 (2014).

111. Niwa, T., Takeuchi, H., Hino, T., Kunou, T. & Kawashima, Y. Preparations of biodegradable nanospheres of water-soluble and insoluble drugs with D,L-lactide/glycolide copolymer by a novel spontaneous emulsification solvent diffusion method, and the drug release behavior. *J. Control. Release* **25,** 89–98 (1993).

112. Lasic, D. D. *Liposomes in Gene Delivery*. 320 (CRC Press, 1997).

113. Malvern Instruments Ltd. Dynamic Light Scattering DLS for particle size characterization of proteins, polymers and colloidal dispersions. (2014). at <http://www.malvern.com/en/products/technology/dynamic-light-scattering/>

114. Jiang, J., Oberdörster, G. & Biswas, P. Characterization of size, surface charge, and agglomeration state of nanoparticle dispersions for toxicological studies. *J. Nanoparticle Res.* **11,** 77–89 (2009).

115. Howell, C. Dynamic Light scattering. *Univ. Sheffield, Polym. Scatt. Gr.* at <http://www.polyshef.co.uk/light-scattering>

116. nanoComposix. *Guidelines for Dynamic Light Scattering Measurement and Analysis* . 1–7 (2012). at <http://nanocomposix.com/sites/default/files/nanoComposix Guidelines for DLS Measurements and Analysis.pdf>

117. *Zetasizer Nano Series User Manual*. 1–270 (2004). at <http://www.biophysics.bioc.cam.ac.uk/files/Zetasizer_Nano_user_manual_Man0317-1.1.pdf>

118. Hollmann, A. *et al.* Characterization of liposomes coated with S-layer proteins from lactobacilli. *Biochim. Biophys. Acta - Biomembr.* **1768,** 393–400 (2007).